Unsymmetrically Bridged Methyl Groups as Intermediates in the Transformation of Bridging Methylene to Bridging Acetyl Groups: Ligand Migrations and Migratory Insertions in Mixed Iridium/Ruthenium Complexes

Rahul G. Samant, Steven J. Trepanier, James R. Wigginton, Li Xu,[‡] Matthias Bierenstiel,[†] Robert McDonald,[§] Michael J. Ferguson,[§] and Martin Cowie*

Department of Chemistry, University of Alberta, Edmonton, Alberta, Canada T6G 2G2

Received February 17, 2009

Protonation of the methylene-bridged, tetracarbonyl species $[IrRu(CO)_4(\mu\text{-}CH_2)(dppm)_2][X]$ (X = CF_3SO_3, BF_4) (**1**) at −90 °C yields the methyl-bridged product $[IrRu(CO)_4(\mu\text{-}CH_3)(dppm)_2][X]_2$ (X = CF_3SO_3, BF_4) (**3**), in which the methyl group is carbon-bound to Ir while engaged in an agostic interaction with Ru. Compound **3** is unusual in that exchange of the terminal and agostic protons of the methyl group is slow on the NMR time scale at −90 °C, allowing for the direct observation of both sets of protons and measurement of their respective C−H coupling constants at this temperature. Protonation of $[IrRu(PMe_3)(CO)_3(\mu\text{-}CH_2)(dppm)_2][CF_3SO_3]$ also yields an unsymmetrically bridged methyl complex, $[IrRu(PMe_3)(CO)_3(\mu\text{-}CH_3)(dppm)_2][CF_3SO_3]_2$ (**7**), analogous to **3**, and again ^1H NMR spectroscopy at temperatures below −60 °C shows separate resonances for the agostic and the terminal hydrogens of the methyl group. Both compounds display very low $^1J_{CH}$ values (65 Hz (**3**); 72 Hz (**7**)) for the agostic interactions, consistent with substantial weakening of the C−H bond. Warming a solution of **3** to −80 °C affords a new species, $[IrRu(CH_3)(CO)_4(dppm)_2][X]_2$ (**4**), in which the methyl group has migrated from the bridging site to a terminal position on Ir. Further warming of the triflate salt of **4** to ambient temperature results in disproportionation to give an unstable tricarbonyl, $[IrRu(CH_3)(CF_3SO_3)(CO)_3(dppm)_2][CF_3SO_3]$ (**6**), that subsequently decomposes, and the pentacarbonyl species $[IrRu(CH_3)(CO)_5(dppm)_2][CF_3SO_3]_2$ (**5**). Compound **5** can be obtained as the sole product upon warming a solution of **4** under an atmosphere of CO. Stirring a solution of **5** for two days gives the migratory-insertion product, $[IrRu(CO)_4(\mu\text{-}C(CH_3)O)(dppm)_2][X]_2$ (**8**), in which the acetyl group is carbon-bound to Ir and oxygen-bound to Ru. One carbonyl ligand can be removed from **8** by reflux in CH_2Cl_2 to give $[IrRu(CO)_3(\mu\text{-}C(CH_3)O)(dppm)_2][BF_4]_2$ (**9**), in the case of **8-BF$_4$**, or $[IrRu(CF_3SO_3)(CO)_3(\mu\text{-}C(CH_3)O)(dppm)_2][CF_3SO_3]$ (**10**), in the case of **8-CF$_3$SO$_3$**, with retention of the bridging acetyl group. Refluxing **8-CF$_3$SO$_3$** in THF removes two carbonyl ligands to give the dicarbonyl species $[IrRu(CF_3SO_3)(CO)_2(\mu\text{-}C(CH_3)O)(dppm)_2][CF_3SO_3]$ (**11**). Reaction of **9** or **10** with H_2 yields the monohydride species $[IrRuH(CO)_3(\mu\text{-}C(CH_3)O)(dppm)_2][X]_2$ (**12**; X = BF_4, CF_3SO_3) via heterolytic cleavage of dihydrogen, while reaction of **11** with H_2 at −90 °C yields the dihydrogen adduct $[IrRu(H_2)(CO)_2(\mu\text{-}C(CH_3)O)(dppm)_2][CF_3SO_3]$ (**13**), which upon warming above −60 °C yields the dihydride $[IrRu(H)_2(CF_3SO_3)(CO)_2(\mu\text{-}C(CH_3)O)(dppm)_2][CF_3SO_3]$ (**14**). Although compound **12** yields acetaldehyde upon reaction with CO, compound **14** gives rise to triflate ion displacement by CO, but no acetaldehyde is formed.

Introduction

Migratory insertion involving metal-bound alkyl and carbonyl groups[1,2] is a pivotal step in a range of important processes including olefin hydroformylation,[3−5] methanol carbonylation,[6−9] and the copolymerization of carbon monoxide and alkenes,[10,11] and may also play a role in the formation of oxygen-containing products in the Fischer−Tropsch (FT) reaction.[12−17] In several of these processes[3−9,12−17] metals of the Co triad play a prominent role. Whereas the FT process is heterogeneously catalyzed and is not yet well understood, the first three processes noted above are homogeneous, have been extensively studied, and are consequently reasonably well understood. Nevertheless, migratory insertion and the influences of the metals and the ancillary ligands on this transformation continue to be of interest.[18,19]

* Corresponding author. E-mail: martin.cowie@ualberta.ca.
‡ Present address: Fujian Institute of Research on the Structure of Matter, Chinese Academy of Science, Fuzhou, Fujian, 350002, People's Republic of China.
† Present address: Department of Chemistry, Cape Breton University, Sydney, Nova Scotia, Canada B1P 6 L2.
§ X-ray Crystallography Laboratory.

(1) Collman, J. P.; Hegedus, L. S.; Norton, J. R.; Finke, R. G. *Principles and Applications of Organotransition Metal Chemistry*; University Science Books: Mill Valley, CA, 1987; Chapter 12.
(2) Niu, S.; Hall, M. B. *Chem. Rev.* **2000**, *100*, 353.
(3) Pruett, R. L. *Adv. Organomet. Chem.* **1979**, *17*, 1.
(4) Pruett, R. L. *Chem. Educ.* **1986**, *63*, 196.
(5) Trzeciak, A. M.; Ziólkowski, J. J. *Coord. Chem. Rev.* **1999**, *190−192*, 883.
(6) Howard, M. J.; Jones, M. D.; Roberts, M. S.; Taylor, S. A. *Catal. Today* **1993**, *18*, 325.
(7) Yoneda, N.; Kusano, S.; Yasui, M.; Pujado, P.; Wilcher, S. *Appl. Catal.* **2001**, *221*, 253.
(8) Haynes, A.; Mann, B. E.; Morris, G. E.; Maitlis, P. M. *J. Am. Chem. Soc.* **1993**, *115* (10), 4093.

10.1021/om900127u CCC: $40.75
Publication on Web 05/28/2009

A recent development in the above carbonyl-insertion processes has been the interest in the cooperative involvement of adjacent metals in both homobinuclear[20,21] and heterobinuclear[5,22−29] systems. In such systems it is clearly of interest to determine the roles of the adjacent metals in the different steps leading to product formation, and in the case of the mixed-metal systems, it is of additional interest to determine at which metal each step occurs. In one particularly interesting study, Komiya and co-workers reported the enhancement of migratory insertion at Pd by an adjacent Co center, and on the basis of DFT calculations a mechanism was proposed in which the roles of the different metals were outlined.[29]

In related studies, involving the Rh/Ru[30] and Rh/Os[31,32] combinations of metals, we have investigated the roles of the different metals in the individual steps leading from bridging methylene groups to bridging acyl groups, using low-temperature multinuclear NMR techniques to study intermediates in the transformation. One of the key steps in this conversion is the formation of a bridging methyl ligand by protonation of the bridging methylene group (see Chart 1). The two most common binding modes for bridging methyl groups are the symmetrically bridged geometry (**A**),[33−45] containing a three-centered M−C−M interaction, and the unsymmetrically bridged geometry (**B**),[30−32,46−52] in which the methyl group is σ-bound to one metal while engaging in a three-centered M−H−C agostic interaction with the other. For late transition metal complexes the unsymmetric mode **B** is by far the more common, with only a few examples reported of species of type **A**.[41−45]

Chart 1

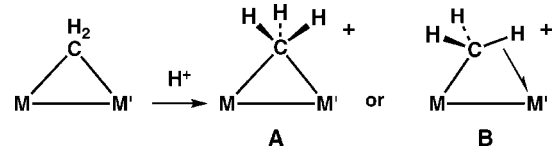

In this paper we extend our previous studies on the Rh/Ru[30] and Rh/Os[31,32] systems to include the Ir/Ru metal combination. We are attempting to obtain a more complete understanding of the roles of different metals in organometallic transformations through studies involving a range of metal combinations, in order to compare the effects of changing from one metal to another.

In addition to complementing our previous work, the Ir/Ru system is particularly relevant to migratory insertion in methanol carbonylation since the CATIVA process[53] utilizes a mixed Ir/Ru catalyst system. Although mechanistic studies have established that the role of Ru in this system is limited to iodide abstraction from Ir, at which all fundamental steps in the process (oxidative addition, migratory insertion, and reductive elimination) appear to occur,[9] the possibility that adjacent Ir and Ru centers could play greater roles in this and related processes is intriguing.

(9) Haynes, A.; Maitlis, P. M.; Morris, G. E.; Sunley, G. J.; Adams, H.; Badger, P. W.; Bowers, C. M.; Cook, D. B.; Elliott, P. I. P.; Ghaffar, T.; Green, H.; Griffin, T. R.; Payne, M.; Pearson, J. M.; Taylor, M. J.; Vickers, P. W.; Watt, R. J. *J. Am. Chem. Soc.* **2004**, *126* (9), 2847.
(10) Selected reviews:(a) Sen, A. *Acc. Chem. Res.* **1993**, *26*, 303. (b) Drent, E.; Budzelaar, P. H. M. *Chem. Rev.* **1996**, *96*, 663. (c) Robertson, R. A. M.; Cole-Hamilton, D. J. C. *Coord. Chem. Rev.* **2002**, *225*, 67. (d) Bianchini, C.; Meli, A.; Oberhauser, W. *Dalton Trans.* **2003**, 2627.
(11) Recent papers:(a) Cavinato, G.; Vavasori, A.; Anadio, E.; Toniolo, L. *J. Mol. Catal. A* **2007**, *278*, 251. (b) Rampersad, M. V.; Zuidema, E.; Ernsting, J. M.; van Leeuwen, P. W. N. M.; Darensbourg, M. Y. *Organometallics* **2007**, *26*, 783. (c) Muñoz-Moreno, B. K.; Claver, C.; Ruiz, A.; Bianchini, C.; Meli, A.; Oberhauser, W. *Dalton Trans* **2008**, 2741.
(12) Watson, P. R.; Somorjai, G. A. *J. Catal.* **1981**, *72*, 347.
(13) Fukushima, T.; Arakawa, H.; Ichikawa, M. *J. Phys. Chem.* **1985**, *89*, 4440.
(14) Fukushima, T.; Arakawa, H.; Ichikawa, M. *J. Chem. Soc., Chem. Commun.* **1985**, 729.
(15) Ichikawa, M. *Polyhedron* **1988**, *7*, 2351.
(16) Shulz, H. *Appl. Catal. A: Gen.* **1999**, *186*, 3.
(17) Overett, M. J.; Hill, R. O.; Moss, J. R. *Coord. Chem. Rev.* **2000**, *206−207*, 581.
(18) Wang, X.; Weitz, E. *J. Organomet. Chem.* **2004**, *689*, 2354.
(19) George, R.; Andersen, J. M.; Moss, J. R. *J. Organomet. Chem.* **1995**, *505*, 131.
(20) Matthews, R. C.; Howell, D. K.; Peng, W.-J.; Train, S. G.; Treheaver, W. D.; Stanley, G. G. *Angew. Chem., Int. Ed. Engl.* **1996**, *35*, 2253.
(21) Broussard, M. E.; Juma, B.; Train, S. G.; Peng, W.-J.; Laneman, S. A.; Stanley, G. G. *Science* **1993**, *260*, 1784.
(22) Hidai, M.; Fukuska, A.; Koyasu, Y.; Uchida, Y. *J. Mol. Catal.* **1986**, *35*, 29.
(23) Hidai, M.; Orisaku, M.; Ue, M.; Koyasu, Y.; Komada, T.; Uchida, Y. *Organometallics* **1983**, *2*, 292.
(24) Fukuska, A.; Fukugawa, S.; Hirano, M.; Komiya, S. *Chem. Lett.* **1997**, 377.
(25) Ishii, Y.; Hidai, M. *Catal. Today* **2001**, *66*, 53.
(26) Van den Beuken, E. K.; Feringa, B. L. *Tetrahedron* **1998**, *54*, 12985.
(27) Komiya, S.; Yasuda, T.; Hirano, A.; Fukuoka, M. *J. Mol. Catal. A: Chem.* **2000**, *159*, 63.
(28) Ishii, Y.; Miyashita, K.; Kamita, K.; Hidai, M. *J. Am. Chem. Soc.* **1997**, *199*, 6448.
(29) Fukuoka, A.; Fukugawa, S.; Hirano, M.; Koga, N.; Komiya, S. *Organometallics* **2001**, *20*, 2065.
(30) Rowsell, B. D.; McDonald, R.; Cowie, M. *Organometallics* **2004**, *23* (16), 3873.
(31) Trepanier, S. J.; McDonald, R.; Cowie, M. *Organometallics* **2003**, *22* (13), 2638.
(32) Wigginton, J. R.; Trepanier, S. J.; McDonald, R.; Ferguson, M. J.; Cowie, M. *Organometallics* **2005**, *24*, 6194.
(33) Byram, S. K.; Fawcett, J. K.; Nyburg, S. C.; O'Brien, R. J. *J. Chem. Soc. D* **1970**, 16.
(34) Evans, W. J.; Anwander, R.; Ziller, J. W. *Organometallics* **1995**, *14* (3), 1107.
(35) Holton, J.; Lappert, M. F.; Scollary, G. R.; Ballard, D. G. H.; Pearce, R.; Atwood, J. L.; Hunter, W. E. *J. Chem. Soc., Chem. Commun.* **1976**, 425.
(36) Holton, J.; Lappert, M. F.; Ballard, D. G. H.; Pearce, R.; Atwood, J. L.; Hunter, W. E. *J. Chem. Soc., Dalton Trans.* **1979**, 54.
(37) Huffman, J. C.; Streib, W. E. *J. Chem. Soc. D* **1971**, 911.
(38) Klooster, W. T.; Lu, R. S.; Anwander, R.; Evans, W. J.; Koetzle, T. F.; Bau, R. *Angew. Chem., Int. Ed. Engl.* **1998**, *37* (9), 1268.
(39) Waezsada, S. D.; Liu, F.-Q.; Murphy, E. F.; Roesky, H. W.; Teichert, M.; Usón, I.; Schmidt, H.-G.; Albers, T.; Parisini, E.; Noltemeyer, M. *Organometallics* **1997**, *16*, 1260.
(40) Yu, Z.; Wittbrodt, J. M.; Heeg, M. J.; Schlegel, H. B.; Winter, C. H. *J. Am. Chem. Soc.* **2000**, *122* (38), 9338.
(41) Beringhelli, T.; D'Alfonso, G.; Panigati, M.; Porta, F.; Mercandelli, P.; Moret, M.; Sironi, A. *J. Am. Chem. Soc.* **1999**, *121*, 2307.
(42) Kruger, C.; Sekutowski, J. C.; Berke, H.; Hoffmann, R. *Z. Naturforsch.* **1978**, *33*, 1110.
(43) Kulzick, M. A.; Price, R. T.; Andersen, R. A.; Muetterties, E. L. *J. Organomet. Chem.* **1987**, *333*, 105.
(44) Reinking, M. K.; Fanwick, P. E.; Kubiak, C. P. *Angew. Chem., Int. Ed. Engl.* **1989**, *28*, 1377.
(45) Schmidt, G. F.; Muetterties, E. L.; Beno, M. A.; Williams, J. M. *Proc. Natl. Acad. Sci. U.S.A.* **1981**, *78*, 1318.
(46) Brookhart, M.; Green, M. L. H. *J. Organomet. Chem.* **1983**, (250), 395.
(47) (a) Brookhart, M.; Green, M. L. H.; Wong, L.-L. *Prog. Inorg. Chem.* **1988**, *36*, 1. (b) Brookhart, M.; Green, M. L. H.; Parkin, G. *Proc. Natl. Acad. Sci. U.S.A.* **2007**, *104*, 6908.
(48) Calvert, R. B.; Shapley, J. R. *J. Am. Chem. Soc.* **1978**, *100* (24), 7726.
(49) Casey, C. P.; Fagan, P. J.; Miles, W. H. *J. Am. Chem. Soc.* **1982**, *104* (4), 1134.
(50) Dawkins, G. M.; Green, M.; Orpen, A. G.; Stone, F. G. A. *J. Chem. Soc., Chem. Commun.* **1982**, 41.
(51) Hursthouse, M. B.; Jones, R. A.; Abdul Malik, K. M.; Wilkinson, G. *J. Am. Chem. Soc.* **1979**, *101* (15), 4128.
(52) Jones, R. A.; Wilkinson, G.; Galas, A. M. R.; Hursthouse, M. B.; Malik, K. M. A. *J. Chem. Soc., Dalton Trans.* **1980**, 1771.
(53) (a) *Chem. Br.* **1996**, *32*, (10) 7. (b) Howard, M. J.; Sunley, G. J.; Poole, A. D.; Watt, R. J.; Sharma, B. K. *Stud. Surf. Sci. Catal.* **1999**, *121*, 61. (c) Sunley, G. J.; Watson, D. J. *Catal. Today* **2000**, *58*, 293. (d) Jones, J. H. *Platinum Met. Rev.* **2000**, *44*, 94. (e) Haynes, A. *Educ. Chem.* **2001**, *38*, 99.

Experimental Section

General Comments. All solvents were dried (using appropriate drying agents), distilled before use, and stored under nitrogen. Reactions were performed under an argon atmosphere using standard Schlenk techniques. $HBF_4 \cdot Me_2O$, CF_3SO_3H, and PMe_3 (1 M in toluene) were purchased from Aldrich. Carbon-13-enriched CO (99.4% enrichment) was purchased from Cambridge Isotopes Laboratories, while hydrogen gas was purchased from Praxair. $[IrRu(CO)_4(\mu\text{-}CH_2)(dppm)_2][BF_4]$ (**1**) and $[IrRu(PMe_3)(CO)_3(\mu\text{-}CH_2)(dppm)_2][BF_4]$ (**2**) were prepared as previously reported.[56] The triflate salt of **1** was prepared by an analogous route using triflic acid instead of tetrafluoroboric acid in the protonation step, and the triflate salt of **2** was prepared by reaction of **1-CF_3SO_3** with PMe_3. NMR spectra were recorded on a Bruker AM-400 spectrometer operating at 400.1 MHz for ^1H, 161.9 MHz for ^{31}P, and 100.6 MHz for ^{13}C nuclei, or a Varian spectrometer operating at 399.9, 161.8, and 100.6 MHz for the respective nuclei. Infrared spectra were obtained on a Nicolet Magna 750 FTIR spectrometer with a NIC-Plan IR microscope. Spectroscopic data for all new compounds are presented in Table 1. The elemental analyses were performed by the microanalytical service within the department. Electrospray mass spectra were run on a Micromass ZabSpec instrument. In all cases the distribution of isotope peaks for the appropriate parent ion matched very closely that calculated for the formulation given.

In all the complexes in which there is no coordinating anion the complex cations involving both the BF_4^- and $CF_3SO_3^-$ salts have identical spectral properties and are therefore interchangeable.

Preparation of Compounds. (a) $[IrRu(CO)_4(\mu\text{-}CH_3)(dppm)_2][CF_3SO_3]_2$ (3). Triflic acid (0.7 μL, 0.0075 mmol) was added to a CD_2Cl_2 solution (0.7 mL) of $[IrRu(CO)_4(\mu\text{-}CH_2)(dppm)_2][CF_3SO_3]$ (**1-CF_3SO_3**) (10 mg, 0.008 mmol) in an NMR tube, cooled to −90 °C using a diethyl ether/liquid nitrogen bath, and monitored with a thermometer. The solution remained yellow; nevertheless, NMR spectra at −90 °C clearly showed the quantitative conversion to a new species (**3**). Compound **3** was unstable, transforming to other species at temperatures above −90 °C, and was therefore characterized by multinuclear NMR techniques at this temperature.

(b) $[IrRu(CH_3)(CO)_4(dppm)_2][CF_3SO_3]_2$ (4). *Method i*: An NMR sample of compound **3** at −90 °C was warmed to −80 °C over a 30 min period. Although the solution remained yellow, the ^1H and ^{31}P NMR spectra indicated the quantitative formation of a new compound (**4**). Again, this product was unstable, transforming to compounds **5** and **6** as the temperature was raised, and was therefore characterized by multinuclear NMR techniques at −80 °C. *Method ii*: Triflic acid as an ethereal solution (1.5 μL in 5 mL, 0.15 mmol) was added to a yellow solution of **1-CF_3SO_3** (20 mg, 0.016 mmol) in 4 mL of CH_2Cl_2 at −78 °C.

(c) Mixture of $[IrRu(CH_3)(CO)_5(dppm)_2][CF_3SO_3]_2$ (5) and $[IrRu(CH_3)(CF_3SO_3)(CO)_3(dppm)_2][CF_3SO_3]$ (6). An NMR sample of compound **4** at −78 °C was gradually warmed to 25 °C. The ^1H and ^{31}P NMR spectra indicated the presence of compounds **4**, **5**, and **6** in a 1:1:1 mixture. Compound **6** did not persist in solution over a 24 h period, decomposing into several unidentified products, so its characterization was based on NMR studies of fresh reaction solutions.

(d) $[IrRu(CH_3)(CO)_5(dppm)_2][CF_3SO_3]_2$ (5). Carbon monoxide was passed through a solution of compound **4** (40 mg, 0.027 mmol) in CH_2Cl_2 (5 mL) at −78 °C for 1 min, resulting in the change of the solution color to a paler shade of yellow. The solution was stirred for 30 min as it was allowed to warm to ambient temperature. Diethyl ether (20 mL) was then added to precipitate a yellow solid. This precipitate was then washed with three 5 mL portions of ether and dried *in vacuo* (yield 86%). Anal. Calcd for $C_{57}H_{47}O_8F_3SP_4IrRu$: C, 45.97; H, 3.13. Found: C, 45.54; H, 3.25. HRMS: *m/z* calcd for $C_{56}H_{46}O_5P_4IrRu$ ($M^+ - H^+ - 2CF_3SO_3^-$) 1217.0968, found 1217.0960. NMR spectra of the redissolved solid showed compound **5** as the only detectable product.

(e) $[IrRu(PMe_3)(CO)_3(\mu\text{-}CH_3)(dppm)_2][CF_3SO_3]_2$ (7). A slight excess of triflic acid (1.4 μL, 0.016 mmol) was added to a CD_2Cl_2 solution (0.7 mL) of $[IrRu(PMe_3)(CO)_3(\mu\text{-}CH_2)(dppm)_2][CF_3SO_3]$ (**2**) (20 mg, 0.014 mmol) in an NMR tube. NMR spectroscopy showed quantitative conversion to a new species (**7**). Precipitation with diethyl ether afforded a yellow solid, which was rinsed with three 5 mL portions of ether before being dried *in vacuo*. Anal. Calcd for $C_{59}H_{56}F_6O_9P_5S_2IrRu$: C, 46.09; H, 3.67. Found: C, 46.37; H, 3.57. HRMS: *m/z* calcd for $C_{57}H_{55}O_3P_5IrRu$ ($M^+ - H^+ - 2CF_3SO_3^-$) 1237.1507, found 1237.1511.

(f) $[IrRu(CO)_4(\mu\text{-}C(CH_3)O)(dppm)_2][CF_3SO_3]_2$ (8). A solution of compound **5** (40 mg, 0.026 mmol) in 10 mL of CH_2Cl_2 was stirred for two days, followed by concentration of the solution to 5 mL under an argon stream. Diethyl ether (20 mL) was added to precipitate a yellow solid, which was collected, washed with three 5 mL portions of ether, and dried *in vacuo* (yield 91%). Spectral characterization of this product showed it to be the only species present. HRMS: *m/z* calcd for $C_{55}H_{47}O_4P_4IrRu$ ($M^{2+} - CO - 2CF_3SO_3^-$) 595.0543, found 595.0543.

(g) $[IrRu(CO)_3(\mu\text{-}C(CH_3)O)(dppm)_2][BF_4]_2$ (9). Compound **8-BF_4** (280 mg, 0.200 mmol) was prepared as described for the preparation of **8-CF_3SO_3**, except using $HBF_4 \cdot OEt_2$ to protonate the BF_4^- salt of **1**. A suspension of **8-BF_4** in CH_2Cl_2 (30 mL) was refluxed for 5 h under an Ar atmosphere. The resulting suspension was filtered, and the red-orange solid was washed with 30 mL of CH_2Cl_2 and 30 mL of pentane and then dried *in vacuo* (yield 70%). Anal. Calcd for $C_{55}H_{47}B_2F_8O_4P_4IrRu$: C, 48.48; H, 3.45. Found: C, 47.96; H, 3.52. MS: *m/z* 595 ($M^+ - 2BF_4^-$).

(h) $[IrRu(OSO_2CF_3)(CO)_3(\mu\text{-}C(CH_3)O)(dppm)_2][CF_3SO_3]$ (10). A solution of 100 mg (0.067 mmol) of compound **8**, as the triflate salt, in 6 mL of CH_2Cl_2 was refluxed for 2 h with a continuous slow stream of argon. The color of the solution changed from yellow to orange. After allowing the solution to cool, diethyl ether (20 mL) and pentane (20 mL) were added to precipitate a pale orange solid, which was washed with three 5 mL portions of ether and dried *in vacuo* (yield 90%). Anal. Calcd for $C_{57}H_{47}F_6O_{10}P_4S_2IrRu$: C, 46.03; H, 3.19. Found: C, 45.64; H, 3.17. MS: *m/z* 595 ($M^{2+} - 2CF_3SO_3^-$).

(i) $[IrRu(OSO_2CF_3)(CO)_2(\mu\text{-}C(CH_3)O)(dppm)_2][CF_3SO_3]$ (11). A slurry of 100 mg (0.067 mmol) of compound **8**, as the triflate salt, in 30 mL of THF was refluxed for 6 h while purging with argon. The color of the solution changed from yellow to red-orange, and a red precipitate formed. After cooling to ambient temperature, diethyl ether (20 mL) was added to fully precipitate the pale red solid. This solid was washed with three 5 mL portions of ether and dried *in vacuo* (yield 88%). Anal. Calcd for $C_{56}H_{47}F_6O_9P_4S_2IrRu$: C, 46.09; H, 3.25. Found: C, 45.68; H, 3.28. MS: *m/z* 581 ($M^{2+} - 2CF_3SO_3^-$).

(j) $[IrRu(H)(CO)_3(\mu\text{-}C(CH_3)O)(dppm)_2][BF_4]$ (12). *Method i:* Compound **9** (100 mg, 0.073 mmol) was suspended in 10 mL of CH_2Cl_2 and H_2 was passed through the mixture for 30 min at a rate of approximately 0.05 mL/s, turning the solution from orange to clear yellow. Ether (50 mL) was added to the solution, affording a yellow precipitate, which was subsequently washed with pentane (2 × 15 mL) and dried *in vacuo* (yield 100%). Anal. Calcd for $C_{55}H_{48}BF_4O_4P_4IrRu$: C, 51.74; H, 3.76. Found: C, 51.19; H, 3.79. MS: *m/z* 1191 ($M^+ - BF_4^-$).

The triflate salt of compound **12** was prepared by an analogous procedure, but starting from compound **10** rather than **9**. *Method ii*: Compound **12-CF_3SO_3** was also prepared through addition of

(54) Siedle, A. R.; Newmark, R. A.; Pignolet, L. H. *Organometallics* **1984**, *3*, 855.
(55) Park, J. W.; Mackenzie, P. B.; Schaefer, W. P.; Grubbs, R. H. *J. Am. Chem. Soc.* **1986**, *108* (20), 6402.
(56) Dell'Anna, M. M.; Trepanier, S. J.; McDonald, R.; Cowie, M. *Organometallics* **2001**, *20*, 88.

Table 1. Spectroscopic Data for the Compounds

compound	IR (cm^{-1})[a]	NMR[bc] $\delta(^{31}P\{^1H\})$[c]	$\delta(^1H)$[d]	$\delta(^{13}C\{^1H\})$[d]
$[IrRu(CO)_4(\mu\text{-}CH_3)(dppm)_2][CF_3SO_3]_2$ (**3**)[e]	N/A	P(Ru): 25.8 (m, 2P) P(Ir): −13.7 (m, 2P)	μ-CH_2H: −10.88 (s, br, 1H); ($^1J_{CH}$ = 65 Hz)[h] μ-CH_2H: 3.79 (m, br, 2H); ($^1J_{CH}$ = 146 Hz)[h] dppm: 4.14 (m, br, 2H), 5.06 (m, br, 2H)	CO(Ir): 170.0 (br, 1C); 161.2 (br, 1C) CO(Ru): 195.6 (br, 1C); 186.0 (br, 1C) CH_3: 18.7 (m, br)
$[IrRu(CH_3)(CO)_4(dppm)_2][CF_3SO_3]_2$ (**4**)[f]	N/A	P(Ru): 20.8 (m, 2P) P(Ir): 18.3 (m, 2p)	CH_3: 2.10 (t, 3H, $^3J_{P(Ir)H}$ = 9 Hz); ($^1J_{CH}$ = 135 Hz)[h] dppm: 3.79 (m, 4H)	CH_3: 39.8 (s, br, 1C) μ-CO: 215.8 (m, 2C) CO(Ru): 187.0 (t, 2C, $^2J_{PC}$ = 9 Hz)
$[IrRu(CH_3)(CO)_5(dppm)_2][CF_3SO_3]_2$ (**5**)	2071(m), 2037(s), 2009(m)	P(Ru): 20.9 (m, 2P), P(Ir): −19.5 (m, 2P)	CH_3: 1.11 (t, br, 3H, $^3J_{P(Ir)H}$ = 5 Hz); ($^1J_{CH}$ = 140 Hz)[h] dppm: 4.58 (m, 4H)	CO(Ru): 202.0 (t, 2C, $^2J_{P(Ru)C}$: 12 Hz); 185.7 (t, 1C, $^2J_{P(Ru)C}$ = 9 Hz) CO(Ir): 181.6 (t, 2C, $^2J_{P(Ir)C}$ = 11 Hz) CH_3: −18.5 (br, t, $^2J_{PC}$ = 3.2 Hz)
$[IrRu(CH_3)(OSO_2CF_3)(CO)_3(dppm)_2][CF_3SO_3]$ (**6**)	2039 (s), 1980 (s), 1784 (m)	P(Ru): 18.0 (m, 2P), P(Ir): 19.8 (m, 2P)	CH_3: 1.58 (t, 3H, $^3J_{P(Ir)H}$ = 8 Hz); ($^1J_{CH}$ = 133 Hz)[h] dppm: 3.42 (m, 2H); 3.08 (m, 2H)	CO(Ru): 222.6 (dt, 1C, $^2J_{P(Ru)C}$ = 11 Hz); 212.4 (m, 1C); 188.4 (m, 1C) CH_3: 33.6 (t; $^2J_{PC}$ = 8 Hz)
$[IrRu(CO)_3(PMe_3)(\mu\text{-}\eta^1\text{:}\eta^2\text{-}CH_3)(dppm)_2]$ $[CF_3SO_3]_2$ (**7**)[g]	2041 (m), 2004 (s)	P(Ru): 18.2 (m, 2P), P(Ir): −17.1 (m, 2P) PMe_3(Ru): −45.7 (m)	μ-CH_2H: −9.09 (br, 1H, $^2J_{HH}$ = 13 Hz); ($^1J_{CH}$ = 72 Hz)[h] μ-CH_2H: 2.93 (br, 2H, $^2J_{HH}$ = 13 Hz,); ($^1J_{CH}$ = 140 Hz)[h] PMe_3: 1.10 (d, 9H, $^2J_{PH}$ = 11 Hz) dppm: 4.13 (m, 2H); 3.87 (m, 2H)	CO(Ru): 203.5 (dt, 1C, $^2J_{P(Ru)C}$ = 10 Hz,; $^2J_{P(Me3)C}$ = 6 Hz); 184.6 (dt, 1C, $^2J_{P(Ru)C}$ = 15 Hz,; $^2J_{P(Me3)C}$ = 18 Hz) CO(Ir): 177.4 (t, 1C, $^2J_{P(Ir)C}$ = 14 Hz) CH_3: (−60 °C) 12.8 (td, $^1J_{CH}$ = 140 Hz, $^1J_{CH}$ = 72 Hz); (−20 °C) 12.9 (q, $^1J_{CH}$ = 117 Hz); (27 °C) 13.0 (q, $^1J_{CH}$ = 133 Hz)
$[IrRu(CO)_4(\mu\text{-}C(CH_3)O)(dppm)_2][CF_3SO_3]_2$ (**8**)	2108(s), 2075(s), 2052(s), 1990(s)	P(Ru): 16.4(m) P(Ir): −17.9(m)	CH_3: 2.43 (s, 3H) dppm: 4.51 (m, 2H); 4.37 (m, 2H)	CH_3CO: 251.2 (m, 1C) CO(Ru): 204.6 (m, 1C); 187.5 (m, 1C) CO(Ir): 172.4 (m, 1C); 157.7 (m, 1C)
$[IrRu(CO)_3(\mu\text{-}C(CH_3)O)(dppm)_2][BF_4]_2$ (**9**)	2017(m), 2002(s), 1961(s)	P(Ru): 19.2(m) P(Ir): 12.5(m)	CH_3: 2.02 (s, 3H) dppm: 4.27 (m, 2H); 3.16 (m, 2H)	CH_3CO: 287.0 (m, 1C) CO(Ru): 206.0 (m, 1C); 179.8 (t, 1C, $^2J_{P(Ru)C}$ = 12 Hz) CO(Ir): 189.0 (m, 1C)
$[IrRu(OSO_2CF_3)(CO)_3(\mu\text{-}C(CH_3)O)(dppm)_2][CF_3SO_3]$ (**10**)	2045(s), 2012(s), 1961(s)	P(Ru): 19.9(m) P(Ir): −14.6(m)	CH_3: 2.46 (s, 3H) dppm: 4.10 (m, 2H); 3.45 (m, 2H)	CH_3CO: 231.4 (s, br,1C) CO(Ru): 205.6 (m, 1C, $^2J_{P(Ru)C}$ = 11 Hz); 186.7 (m, 1C, $^2J_{P(Ru)C}$ = 15 Hz) CO(Ir): 168.6 (s, br,1C)
$[IrRu(OSO_2CF_3)(CO)_2(\mu\text{-}C(CH_3)O)(dppm)_2][CF_3SO_3]$ (**11**)	2041(s), 1988(s)	P(Ru): 18.0(m) P(Ir): 15.1(m)	CH_3: 1.57 (s, 3H) dppm: 3.73 (m, 2H); 2.45 (m, 2H)	CH_3CO: 231.4 (t,1C, $^2J_{P(Ir)C}$ = 4 Hz) CO(Ru): 205.6 (t, 1C, $^2J_{P(Ru)C}$ = 11 Hz); 186.7 (m, 1C, $^2J_{P(Ru)C}$ = 15 Hz)
$[IrRu(H)(CO)_3(\mu\text{-}C(CH_3)O)(dppm)_2][CF_3SO_3]$ (**12**)	2070(m), 2010(s), 1966(s)	P(Ru): 27.0 (m) P(Ir): 0.8 (m)	CH_3: 1.22 (s, 3H) dppm: 3.95 (m, 4H) H: −10.35 (t,1H, $^2J_{P(Ir)H}$ = 12 Hz)	CH_3CO: 260.2 (dm, 1C, $^2J_{CC}$ = 30 Hz) CO(Ru): 212.0 (t, 1C, $^2J_{P(Ru)C}$ = 10 Hz); 188.0 (t, 1C, $^2J_{P(Ru)C}$ = 12 Hz) CO(Ir): 183.4 (dm, 1C, $^2J_{CC}$ = 30 Hz)
$[IrRu(CO)_2(H_2)(\mu\text{-}C(CH_3)O)(dppm)_2][CF_3SO_3]_2$ (**13**)[e]	N/A	16.0 (m, br)	CH_3: 1.52 (s, 3H) dppm: 3.67 (m, 2H); 2.37 (m, 2H) H_2: −0.03 (br, 2H)	CH_3CO: 211.8 (m, 1C) CO(Ru): 203.1 (m, 1C, $^2J_{P(Ru)C}$ = 13 Hz); 202.5(t, 1C, $^2J_{P(Ru)C}$ = 11 Hz)
$[IrRu(H)_2(OSO_2CF_3)(CO)_2(\mu\text{-}C(CH_3)O)(dppm)_2][CF_3SO_3]$ (**14**)	2040(s) 1992(s)	P(Ru): 15.3 (m) P(Ir): 10.4 (m)	CH_3: 0.94 (s, 3H) dppm: 6.18 (m, 2H); 4.88 (m, 2H) H: −12.28 (m, 1H, $^2J_{P(Ir)H}$ = 12 Hz; $^3J_{HH}$ = 5 Hz) H: −9.95 (m, 1H, $^2J_{P(Ru)H}$ = 3 Hz; $^3J_{HH}$ = 5 Hz, $^4J_{HH(dppm)}$ = 3 Hz)	CH_3CO: 235.6 (t, 1C, $^2J_{P(Ir)C}$ = 5 Hz) CO(Ru): 192.8 (tm, 1C, $^2J_{P(Ru)C}$ = 14 Hz); 191.8 (m, 1C) (t, 1C, $^2J_{P(Ru)C}$ = 8.8 Hz);
$[IrRu(H)_2(CO)_3(\mu\text{-}C(CH_3)O)(dppm)_2][CF_3SO_3]_2$ (**15**)	2015(s) 2022(s) 1963(s)	P(Ru): 16.9 (m) P(Ir): −10.8 (m)	CH_3: 2.27 (s, 3H) dppm: 4.86 (m, 2H); 4.14 (m, 2H)) H: −13.42 (br, 1H); −12.40 (br, 1H)	CO(Ru): 194.2 (t, 1C, $^2J_{P(Ru)C}$ = 10.6 Hz); 190.2 (m, 1C) CO(Ir): 167.3 (td, 1C, $^2J_{P(Ir)C}$ = 10.5 Hz), $^2J_{CC}$ = 4.4 Hz); C(O)CH_3: 262.0 (m, 1C, $^2J_{CC}$ = 4.4 Hz)

[a] IR abbreviations: s = strong, m = medium, br = broad. Dichloromethane solution: in units of cm^{-1}. [b] NMR abbreviations: s = singlet, d = doublet, t = triplet, m = multiplet, br = broad, bs = broad singlet, bd = broad doublet. NMR data at 27 °C in CD_2Cl_2 unless otherwise indicated. [c] ^{31}P chemical shifts referenced to external 85% H_3PO_4. [d] ^1H and ^{13}C chemical shifts referenced to TMS. Chemical shifts for the phenyl protons are not given; the labeled dppm are for the methylene groups. [e] NMR data in CD_2Cl_2 at −90 °C. [f] NMR data in CD_2Cl_2 at −40 °C. [g] NMR data in CD_2Cl_2 at −60 °C [h] $^{13}CH_3$-enriched sample.

Table 2. Crystallographic Data for Compounds 5, 8, 9, and 11

	$[IrRu(CH_3)(CO)_5(dppm)_2][CF_3SO_3]_2$ (**5**)·$3CH_2Cl_2$	$[IrRu(CO)_4(\mu\text{-}C(CH_3)O)(dppm)_2][BF_4]_2$ (**8**)·$3CH_2Cl_2$	$[IrRu(CO)_3(\mu\text{-}C(CH_3)O)(dppm)_2][BF_4]_2$ (**9**)·$3CH_2Cl_2$	$[IrRu(CF_3SO_3)(CO)_2(\mu\text{-}C(CH_3)O)(dppm)_2][CF_3SO_3]$ (**11**)·$2CH_2Cl_2$
formula	$C_{61}H_{53}Cl_6F_6IrO_{11}P_4RuS_2$	$C_{59}H_{53}B_2Cl_6F_8IrO_5P_4Ru$	$C_{58}H_{53}B_2Cl_6F_8O_4P_4Ru$	$C_{58}H_{51}Cl_4F_6IrO_9P_4RuS_2$
fw	1770.00	1645.48	1617.47	1629.06
cryst dimens, mm	0.57 × 0.11 × 0.04	0.23 × 0.10 × 0.08	0.24 × 0.24 × 0.06	0.26 × 0.16 × 0.04
cryst syst	monoclinic	monoclinic	monoclinic	orthorhombic
space group	*Cc* (No. 9)	*C*2/*c* (No. 15)	$P2_1/c$ (No. 14)	$P2_12_12_1$ (No. 19)
a, Å	11.3730(8)[a]	37.384(3)[b]	18.899(3)[c]	14.609(1)[d]
b, Å	35.712(2)	14.505(1)	14.728(3)	17.007(1)
c, Å	16.776(1)	23.947(2)	24.634(4)	24.688(2)
β, deg	95.644(1)	99.127(2)	112.097(3)	90
V, Å^3	6780.7(8)	12821(2)	6353(2)	6133.9(9)
Z	4	8	4	4
d_{calcd}, *g cm*$^{-3}$	1.734	1.705	1.691	1.764
μ, mm^{-1}	2.649	2.730	2.752	2.834
radiation (λ, Å)	graphite-monochromated Mo Kα (0.71073)			
T, °C	−80	−80	−80	−80
scan type	ω scans (0.2°) (15 s exposures)	ω scans (0.2°) (25 s exposures)	ϕ rotations (0.3°)/ω scans (0.3°) (30 s exposures)	ω scans (0.2°) (30 s exposures)
2θ(max), deg	52.78	52.78	52.90	52.80
no. of unique rflns	13 742 (R_{int}=0.0460)	13011 (R_{int}=0.0742)	13001 (R_{int}=0.0695)	12 557 (R_{int} = 0.0782)
no. of observns	11 689 ($F_o^2 \geq 2\sigma(F_o^2)$)	8788 ($F_o^2 \geq 2\sigma(F_o^2)$)	7896 ($F_o^2 \geq 2\sigma(F_o^2)$)	10 244 ($F_o^2 \geq 2\sigma(F_o^2)$)
range of transmn factors	0.9014−0.3135	0.8112−0.5725	0.8310−0.5203	0.8951−0.5262
no. of data/restraints/params	13 742 ($F_o^2 \geq -3\sigma(F_o^2)$)/18/838	13 011 ($F_o^2 \geq -3\sigma(F_o^2)$)/4/763	13 001 ($F_o^2 \geq -3\sigma(F_o^2)$)/0/758	12 557 ($F_o^2 \geq -3\sigma(F_o^2)$)/0/768
residual density, e/Å^3	1.037 and −0.817	2.191 and −0.858	3.71 and −3.108	1.446 and −1.047
R_1 ($F_o^2 \geq 2\sigma(F_o^2)$)	0.0413	0.0516	0.0560	0.0418
wR_2 ($F_o^2 \geq -3\sigma(F_o^2)$)	0.0913	0.1159	0.1499	0.0943
GOF (s)	1.010	1.003	0.968	1.026

[a] Cell parameters obtained from least-squares refinement of 4551 centered reflections. [b] Cell parameters from 5570 reflections. [c] Cell parameters from 5177 reflections. [d] Cell parameters from 4777 reflections. [e] $R_1 = \sum|F_o| - |F_c|/\sum|F_o|$; $wR_2 = [\sum w(F_o^2 - F_c^2)^2/\sum w(F_o^4)]^{1/2}$. [f] $S = [\sum w(F_o^2 - F_c^2)^2/(n-p)]^{1/2}$ (n = number of data; p = number of parameters varied; $w = [\delta^2(F_o^2) + (a_oP)^2 + a_1P]^{-1}$, where $P = [\max(F_o^2, 0) = 2F_c^2]/3$). For **4** $a_o = 0.0260$ and $a_1 = 5.3436$; for **6** $a_o = 0.0496$ and $a_1 = 2.2684$; for **7** $a_o = 0.0778$ and $a_1 = 0.0$; for **9** $a_o = 0.0433$ and $a_1 = 0.0$.

superhydride ($LiBEt_3H$) (1 M in THF) (2 μL, 0.015 mmol) to a THF solution (10 mL) of **10** (20 mg, 0.015 mmol) at ambient temperature. After 10 min diethyl ether (30 mL) was slowly added to precipitate a pale yellow solid. ^{31}P NMR spectroscopy showed quantitative conversion to **12**.

(k) $[IrRu(H_2)(CO)_2(\mu\text{-}C(CH_3)O)(dppm)_2][CF_3SO_3]_2$ (13). A CD_2Cl_2/CD_3NO solution (0.65 mL/0.05 mL) of compound **11** (10 mg, 0.007 mmol) was cooled to −90 °C and then saturated with H_2. Approximately 50% of compound **11** was converted to **13**, along with numerous other decomposition products. Compound **13** was characterized by NMR spectroscopy at −90 °C since it converted back to **11** at higher temperatures and formed compound **14** above −60 °C. Removal of H_2 by vacuum or an Ar stream at −90 °C also resulted in the conversion of **13** into **11**.

(l) $[IrRu(H)_2(OSO_2CF_3)(CO)_2(\mu\text{-}C(CH_3)O)(dppm)_2][CF_3SO_3]$ (14). Compound **11** (20 mg, 0.014 mmol) was dissolved in 10 mL of CH_2Cl_2 at ambient temperature, and H_2 was passed through the yellow solution for 5 min at a rate of 0.05 mL/s. The solution was stirred for a further 30 min, after which diethyl ether (20 mL) and pentane (20 mL) were added to precipitate a pale yellow solid. The solid was washed with three 5 mL aliquots of ether and dried *in vacuo* (yield 90%). Anal. Calcd for $C_{56}H_{55}O_9F_6P_4S_2IrRu$: C, 45.77; H, 3.78. Found: C, 46.05; H, 4.26.

(m) $[IrRu(H)_2(CO)_3(\mu\text{-}C(CH_3)O)(dppm)_2][CF_3SO_3]_2$ (15). Carbon monoxide was passed through a solution of **14** (20 mg, 0.014 mmol) in 2 mL of CH_2Cl_2 at a rate of 0.1 mL/s for 2 min. ^{31}P NMR confirmed complete conversion of **14** to **15**. The solution volume was reduced to 50% *in vacuo*, and the addition of 5 mL of ether afforded a yellow powder, which was rinsed three times with 1 mL portions of ether before being dried *in vacuo* (yield 85%). HRMS: *m*/*z* calcd 596.0627 ($M^{2+} - 2(CF_3SO_3)$), found 596.0635.

(n) Reaction of 12 with CO. Carbon monoxide was passed through a solution of **12** (15 mg, 0.010 mmol) in 0.7 mL of CD_2Cl_2 at a rate of 0.1 mL/s for 2 min. ^{31}P NMR of the sample revealed the formation of previously known species $[IrRu(CO)_4(dppm)_2][CF_3SO_3]$ accompanied by numerous unknown decomposition products (approximately 50% of all phosphorus-containing products based on integration of the $^{31}P\{^1H\}$ NMR spectra), whereas ^1H NMR of the sample showed approximately 0.2 equiv of acetylaldehyde.

X-ray Data Collection and Structure Solution. (a) Pale yellow crystals of $[IrRu(CH_3)(CO)_5(dppm)_2][CF_3SO_3]_2 \cdot 3CH_2Cl_2$ (**5**) were obtained via slow diffusion of diethyl ether into a dichloromethane solution of the compound. Data were collected on a Bruker PLATFORM/SMART 1000 CCD diffractometer[57] using Mo Kα radiation at −80 °C. Unit cell parameters were obtained from a least-squares refinement of the setting angles of 4551 reflections from the data collection. The space group was determined to be *Cc* (No. 9). Data were corrected for absorption through use of the SADABS procedure. See Table 2 for a summary of crystal data and X-ray data collection information.

The structure of **5** was solved using the Patterson search and structure expansion routines as implemented in the DIRDIF-99[58] program system. Refinement was completed using the program SHELXL-93.[59] Hydrogen atoms were assigned positions based on the geometries of their attached carbon atoms and were given thermal parameters 20% greater than those of the attached carbons. The metal atom sites were found to be disordered; the atom labeled Ir in Figure 1 was refined as a combination of 60% Ir and 40% Ru, while the Ru atom was refined at 60% Ru and 40% Ir. The iridium-bound methyl group and the carbonyl group attached to ruthenium trans to iridium (C(6)O(6) in Figure 1) were likewise disordered, with O(6) and the hydrogens attached to C(3) refined with an occupancy factor of 60% (the oxygen attached to C(3) and the hydrogens on the minor-occupancy species, attached to C(6), were refined at 40% occupancy). One of the triflate counterions was also disordered, resulting in the splitting of its fluorine, oxygen, and carbon atoms into two sets of equally abundant positions sharing the same sulfur atom. The final model for **5** was refined to values of $R_1(F) = 0.0413$ (for 11 689 data with $F_o^2 \geq 2\sigma(F_o^2)$) and $wR_2(F^2) = 0.0913$ (for all 13 742 independent data).

(57) Programs for diffractometer operation, data collection, data reduction, and absorption correction were those supplied by Bruker.

(58) Beurskens, P. T.; Beurskens, G.; de Gelder, R.; Garcia-Granda, S.; Isreal, R.; Gould, R. O.; Smits, J. M. M. The DIRDIF-99 program system; Crystallography Laboratory, University of Nijmegen, The Netherlands, 1999.

(59) Sheldrick, G. M. *SHELXL-93, Program for Crystal Structure Determination*; University of Göttingen: Germany, 1993.

Scheme 1

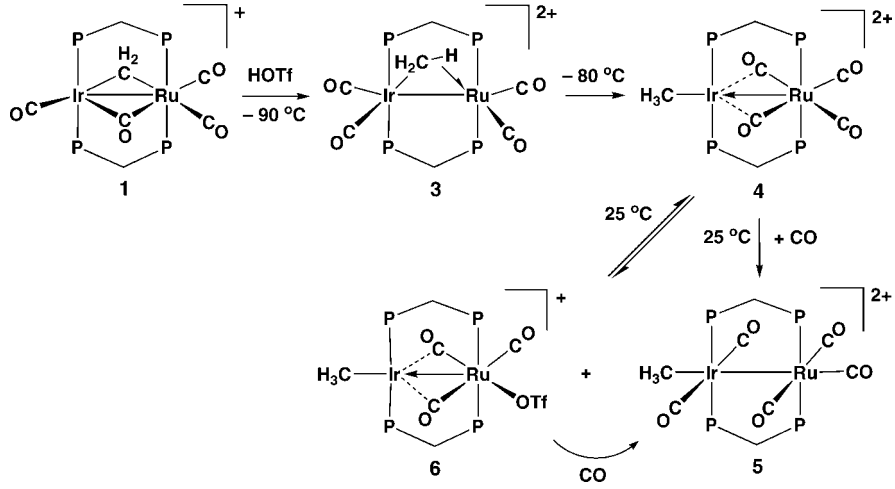

(b) Colorless crystals of $[IrRu(CO)_4(\mu\text{-}C(CH_3)O)(dppm)_2][BF_4]_2 \cdot 3CH_2Cl_2$ (**8-BF$_4$**) were obtained via slow evaporation of a dichloromethane solution of the compound. Data were collected and corrected for absorption as for **5** above (see Table 2). Unit cell parameters were obtained from a least-squares refinement of the setting angles of 5570 reflections from the data collection, and the space group was determined to be *C*2/*c* (No. 15). The structure of **8-BF$_4$** was solved using the direct-methods program SHELXS-86,[60] and refinement was completed using the program SHELXL-93, during which the hydrogen atoms were treated as for **5**. For **8-BF$_4$** the Cl−C distances within one of the solvent dichloromethane molecules (containing a carbon atom that was disordered over two positions) were given a fixed idealized value (1.80 Å). The final model was refined to values of $R_1(F) = 0.0516$ (for 8788 data with $F_o^2 \geq 2\sigma(F_o^2)$) and $wR_2(F^2) = 0.1159$ (for all 13 011 independent data).

(c) Red-orange crystals of $[IrRu(CO)_3(\mu\text{-}C(CH_3)O)(dppm)_2][BF_4]_2 \cdot 3CH_2Cl_2$ (**9**) were obtained via slow evaporation of a dichloromethane solution of the compound. Data were collected on a Bruker P4/RA/SMART 1000 CCD diffractometer using Mo Kα radiation at −80 °C and corrected for absorption as for **5** above (see Table 2). Unit cell parameters were obtained from a least-squares refinement of the setting angles of 5177 reflections from the data collection, and the space group was determined to be $P2_1/c$ (No. 14). The structure of **9** was solved as for **5** (DIRDIF-99), and refinement was completed using the program SHELXL-93, during which the hydrogen atoms were treated as for **5**. The final model was refined to values of $R_1(F) = 0.0560$ (for 7896 data with $F_o^2 \geq 2\sigma(F_o^2)$) and $wR_2(F^2) = 0.1499$ (for all 13 001 independent data).

(d) Crystals of $[IrRu(O_3SCF_3)(CO)_2(\mu\text{-}C(CH_3)O)(dppm)_2][CF_3SO_3] \cdot 2CH_2Cl_2$ (**11**) were obtained as orange plates from a dichloromethane solution of the compound. Data were collected and corrected for absorption as for **5**. Unit cell parameters were obtained from a least-squares refinement of the setting angles of 4777 reflections from the data collection, and the space group was determined to be $P2_12_12_1$ (No. 19). The structure of **11** was solved as for **5** (DIRDIF-99), and refinement was completed using the program SHELXL-93, during which the hydrogen atoms were treated as for **5**. The final model was refined to values of $R_1(F) = 0.0418$ (for 10 244 data with $F_o^2 \geq 2\sigma(F_o^2)$) and $wR_2(F^2) = 0.0943$ (for all 12 557 independent data).

Results and Discussion

(a) Methyl Complexes. In our previous studies on the Rh/Os[31] and Rh/Ru[30] systems, protonation of the methylene-bridged complexes $[RhM(CO)_4(\mu\text{-}CH_2)(dppm)_2]^+$ (M = Ru, Os) at temperatures below −40 °C yielded methyl-bridged products $[RhM(CO)_4(\mu\text{-}CH_3)(dppm)_2]^{2+}$, in which the methyl group in each case was carbon-bound to the group 8 metal while being involved in an agostic interaction with Rh. Even at temperatures down to −90 °C no metal hydride species was observed in these protonation reactions, suggesting direct protonation of the methylene group. We undertook the present study, in part, to determine whether a metal hydride species could be observed. The greater propensity of Ir over Rh for C−H bond activation and the greater Ir−C and Ir−H bond strengths[61] suggested that the methylene/hydride species may be favored in this system over the bridged, agostic methyl product.

Protonation of the methylene-bridged compound $[IrRu(CO)_3(\mu\text{-}CH_2)(\mu\text{-}CO)(dppm)_2][CF_3SO_3]$ (**1**) at −90 °C using triflic acid yields the dicationic methyl-bridged product, $[IrRu(CO)_4(\mu\text{-}CH_3)(dppm)_2][CF_3SO_3]_2$ (**3**) as outlined in Scheme 1. The $^{31}P\{^1H\}$ NMR spectrum of **3** displays a pattern that is typical for these dppm-bridged species,[56] corresponding to an AA′BB′ spin system, in which the Ru-bound ^{31}P nuclei appear as a multiplet at lower field (δ 25.8) than those bound to Ir (δ −13.7). The ^1H resonances for the methyl group at −90 °C appear as two broad unresolved signals; the resonance at δ −10.88 integrates as one proton, while that at δ 3.79 integrates as two. Although the chemical shifts of these resonances are suggestive of metal-bound hydride and methylene groups, respectively, a bridged agostic methyl interaction has been established on the basis of the $^1J_{CH}$ values observed in the sample prepared using $^{13}CH_2$-enriched compound **1**. In this experiment the high-field proton signal shows a coupling of 65 Hz to carbon, while the resonance for the other pair of protons displays a coupling of 146 Hz. The former coupling is far too large to correspond to coupling between separate hydride and methylene groups, while the latter coupling is somewhat larger than the normal range observed for terminal methyls (120−135 Hz). This latter coupling is in line with what has been observed for the terminal C−H moieties in agostic alkyl groups[46,47] and has been attributed to the increase in s-character in these nonbridging bonds.[46] It should also be noted that values of $^1J_{CH}$, close to what we observe for the low-field methyl protons in **3**, have also been reported for some terminally bound methyl groups.[8,54]

(60) Sheldrick, G. M. *Acta Crystallogr.* **1990**, *A46*, 467.

(61) (a) Ziegler, T.; Tschinke, V. In *Bonding Energetics in Organometallic Compounds*; Marks, T. J., Ed.; ACS: Washington, DC, 1990; Chapter 19. (b) Ziegler, T.; Tschinke, V.; Ursenbach, B. *J. Am. Chem. Soc.* **1987**, *109*, 4825. (c) Armentrout, P. B. In *Bonding Energetics in Organometallic Compound*; Marks, T. J., Ed.; ACS: Washington, DC, 1990; Chapter 2.

The observation of separate signals for the hydrogen involved in the agostic interaction and the two terminal hydrogens, and therefore the direct observation of both C−H coupling constants, is highly unusual. In general, exchange of the three methyl hydrogens is facile on the NMR time scale, even at low temperature, giving rise to only a single ^{1}H resonance displaying a splitting that corresponds to the weighted average of the two coupling constants.[30−32,46,47] We are aware of only one previous example in which both the agostic and terminal C−H resonances for a bridging methyl group have been resolved,[55] for which the agostic interaction displays a C−H coupling constant of 88 Hz. The very low value of $^1J_{CH}$ observed in **3** suggests a very strong agostic interaction in this case and a concomitant, substantially weakened C−H bond. This value also lies in the range of 50 to 100 Hz that has been reported for agostic interactions involving bridging, substituted alkyl groups.[46,47] No spin−spin coupling between the chemically inequivalent protons could be resolved, owing to the breadth of both the high- and low-field signals (35 and 25 Hz, respectively), even upon broadband ^{31}P decoupling. The bridging methyl group in **3** is proposed, on the basis of selective ^{31}P-decoupling experiments, to have the connectivity shown in Scheme 1, in which it is carbon-bound to Ir with the agostic interaction with Ru. Although both methyl signals in the ^{1}H NMR spectrum are broad and unresolved, decoupling the phosphorus resonance corresponding to the Ru-bound ends of the dppm ligands results in a slight sharpening of the high-field methyl resonance (δ −10.88), while decoupling of the Ir-bound ends of the diphosphines has no effect on this signal. Conversely, the ^{1}H methyl signal at δ 3.79 sharpens slightly on decoupling the Ir-bound phosphine signal but is unaffected by decoupling of the Ru-bound phosphine signal. In a $^{13}CH_3$-enriched sample of **3** the broad signal in the $^{13}C\{^1H\}$ NMR spectrum at δ 18.7 for this methyl group sharpens on ^{31}P decoupling of the Ir-bound phosphorus nuclei, but remains unaffected when the Ru-bound phosphorus resonance is decoupled. This again supports the structure shown in Scheme 1.

Unfortunately, the connectivity involving the carbonyl ligands could not be unambiguously established through selective ^{31}P-decoupling experiments owing to the breadth of the carbonyl signals in the $^{13}C\{^1H\}$ NMR spectra, which remained unaffected during all ^{31}P-decoupling experiments. Nevertheless, the connectivity could be established with some confidence on the basis of the chemical shifts of these carbonyls. Two carbonyl resonances appear at relatively high field (δ 161.2, 170.0) and are assumed to be bound to Ir, while the two lower field resonances (δ 186.0, 195.6) are assumed to be Ru-bound; such high- and low-field signals for carbonyls bound to third- and second-row metals, respectively, have previously been observed in Ir/Ru complexes[56] and in related mixed-metal complexes involving other combinations of second- and third-row transition metals.[31,32,62] Although all chemical shifts appear to be consistent with terminally bound carbonyls, the lowest field resonance may correspond to a carbonyl having some weak semibridging interaction with the adjacent metal.

Warming a solution of **3** only slightly to −80 °C for 30 min results in complete conversion to a new product, $[IrRu(CH_3)(CO)_4(dppm)_2][CF_3SO_3]_2$ (**4**), in which the bridging methyl group of **3** has migrated to a terminal site on Ir. Although, as noted above, in previous work,[56] and in some of what follows, the Ir-bound ^{31}P nuclei usually appear at significantly higher field in the $^{31}P\{^1H\}$ NMR spectra than those bound to Ru, aiding significantly in the spectroscopic characterization of the compounds, this is not the case for **4** (and for some other compounds in this paper), for which the pair of ^{31}P resonances appear at very similar chemical shifts (δ 20.8 and 18.3). The close proximity of these two resonances leads to some equivocation in structural assignment since the Ir- and Ru-bound ^{31}P resonances cannot be unambiguously distinguished. However, if it is assumed that the ^{31}P signal at slightly higher field corresponds to the Ir-bound ends of the diphosphines, the resulting structural assignment for this species is more consistent with those of the subsequent products and with the geometries established for the analogous Rh/Os[31] and Rh/Ru[30] compounds. In the ^{1}H NMR spectrum of **4** a resonance corresponding to a methyl group appears as a triplet at δ 2.10, and selective ^{31}P decoupling confirms that its multiplicity results from coupling to the ^{31}P nuclei appearing at higher field. On the basis of our assumption above, this suggests that the methyl group is also Ir-bound. This assignment is consistent with that of the subsequent product **5**, for which the methyl group is clearly bound to Ir (*vide infra*). In a $^{13}CH_3$-enriched sample of **4** the value of $^1J_{CH}$ = 135 Hz is found to be as expected for a terminally bound methyl group. Also in the ^{1}H NMR spectrum all four dppm methylene protons appear as a single resonance at δ 3.79, suggesting front−back symmetry of the complex on either side of the $IrRuP_4$ plane. Two carbonyl resonances appear in the $^{13}C\{^1H\}$ NMR spectrum; one at δ 187.0 corresponds to the pair that are terminally bound to Ru, while the low-field signal at δ 215.8 represents a pair of semibridging carbonyls. These assignments are based on a series of $^{13}C\{^{31}P\}$ decoupling experiments in which the low-field carbonyl signal shows coupling to all ^{31}P nuclei, while the high-field signal couples only to the ^{31}P nucleus resonating at low-field. These ^{13}CO resonances also closely resemble those of the RhRu[30] analogue. The methyl group of compound **4** appears as a broad signal at δ 39.8 in the $^{13}C\{^1H\}$ NMR spectrum, and ^{31}P decoupling experiments result in sharpening of this signal only on decoupling the Ir-bound phosphines.

The proposed connectivity for **4** is similar to those reported for the Rh/Os[31] and Rh/Ru[30] analogues, the spectral characterization of which was unambiguous owing to the presence of spin−spin coupling involving the ^{103}Rh nuclei in these cases. Although we describe the connectivity with some confidence on the basis of the spectral data, the oxidation states of the metals and the resulting nature of the Ir−Ru bond remain equivocal; such a situation is common in binuclear complexes. In our structural assignment for **4**, shown in Scheme 1, we assume Ir^{1+}/Ru^{2+} oxidation states, necessitating a dative Ru→Ir bond.

The bonding of the bridging methyl group in **3** is subtly different from that observed in the Rh/Os and Rh/Ru analogues. Whereas the methyl group in **3** is carbon-bound to Ir and binds to Ru via an agostic interaction, the reverse is true in the Rh systems,[30−32] in which the methyl group is bound to the group 8 metal while having an agostic interaction with Rh. We assume that this difference reflects the stronger Ir−CH_3 vs Ru−CH_3 bond[61] in **3**. Our proposal that the primary metal−carbon interaction in **3** is to Ir is also consistent with the significantly more facile bridging methyl-to-terminal methyl transformation (**3** → **4**) that occurs upon warming only slightly to −80 °C; the analogous transformation for both the Rh/Os and Rh/Ru systems required warming to −40 °C. The higher barrier for the latter two cases is consistent with the necessity of the methyl group to migrate from metal to metal, breaking both the agostic interaction and the Os−CH_3 or Ru−CH_3 sigma bonds, before the partial "merry-go-round" motion takes it to its favored

(62) George, D. S. A.; McDonald, R.; Cowie, M. *Organometallics* **1998**, *17*, 2553.

terminal site on the group 9 metal. By contrast, migration of the methyl group in the conversion of **3** to **4** requires only breaking of the weaker agostic interaction while maintaining the strong Ir−CH_3 bond.

Warming a solution of **4** (as the triflate salt) to −60 °C results in the gradual appearance of two new species (**5** and **6**) in equal proportions, and warming to −20 °C for 30 min gives rise to an equilibrium mixture of compounds **4**, **5**, and **6** in an approximate 1:1:1 ratio. However, species **6** is unstable and begins decomposing into unidentified products within hours, ultimately leaving only $[IrRu(CH_3)(CO)_5(dppm)_2][CF_3SO_3]_2$ (**5**) and unidentified decomposition products. This latter species can be obtained as the sole product upon reaction of either **4** or a mixture of **4**, **5**, and **6** with carbon monoxide and is the only product obtained upon ambient-temperature protonation of **1** under carbon monoxide. The $^{31}P\{^1H\}$ NMR spectrum of **5** displays the conventional AA′BB′ pattern in which the Ir-bound ^{31}P nuclei appear at high field (δ −19.5), while those bound to Ru are at characteristically lower field (δ 20.9). In the ^1H NMR spectrum a methyl signal appears at δ 1.11, and its coupling to the high-field ^{31}P nuclei was confirmed by ^{31}P-decoupling experiments. In the $^{13}CH_3$-enriched sample a value for $^1J_{CH}$ = 140 Hz was observed. Three carbonyl resonances, in a 2:2:1 ratio, appear in the $^{13}C\{^1H\}$ NMR spectrum, and their connectivity was also established by decoupling experiments; a triplet at δ 181.6 corresponds to two equivalent Ir-bound carbonyls, a triplet at δ 202.0 represents two equivalent Ru-bound carbonyls, and a triplet at δ 185.7 corresponds to a single unique carbonyl on Ru. In addition, the methyl resonance in the $^{13}CH_3$-enriched sample appears as a partially resolved triplet ($^2J_{PC}$ = 3.2 Hz) at δ −18.5, and selective ^{31}P decoupling establishes that this group is bound to Ir. The structure proposed for **5** is analogous to that proposed for the isoelectronic diruthenium species $[Ru_2(CH_3)(CO)_5(dmpm)_2][CF_3SO_3]$ (dmpm = $Me_2PCH_2PMe_2$)[63] and has been confirmed by an X-ray structure determination. A representation of the complex cation is shown in Figure 1. Although the structure has a disordered "H_3C−Ir−Ru−CO" fragment as explained in the Experimental Section, the location of the methyl group on Ir and the unique carbonyl on Ru was established on the basis of the different occupancy factors for the disordered atoms. Both metals have a relatively undistorted octahedral geometry, in which one coordination site on each is occupied by the bond to the adjacent metal. The resulting Ir−Ru separation (2.9143(5) Å) is long for a single bond, reflecting the repulsions between the two pairs of carbonyls on the adjacent metals that lie cis to the Ir−Ru bond, and is certainly longer than those observed for compounds **8**, **9**, and **11** (*vide infra*). Nevertheless, this metal−metal distance is less than the intraligand P−P separations (3.092(2), 3.097(3) Å), consistent with a mutual attraction of the metals and the presence of a metal−metal bond. The repulsions between adjacent ligands on both metals are further manifested in a staggering of the two adjoining octahedra by approximately 26.8°, as can be seen in Figure 1. All bond lengths and angles within the complex cation appear to be normal, although the disorder, noted above, means that the precise location of the methyl group and the axial carbonyl on Ru cannot be determined, so the metrical parameters involving these groups must be viewed with caution.

The $^{31}P\{^1H\}$ NMR spectrum of the other product in the transformation of **4**, namely, $[IrRu(CH_3)(OSO_2CF_3)(CO)_3(dppm)_2][CF_3SO_3]$ (**6**), shows that, like **4**, it is atypical, having two closely spaced resonances at δ 19.8 and 18.0. In this case it also appears that the slightly higher field chemical shift corresponds to the phosphorus nuclei bound to Ru. The similarity in the chemical shifts of these resonances to those of **4** suggests that the two may have similar structures. Compound **6** is shown, by its $^{13}C\{^1H\}$ NMR spectrum, to be a tricarbonyl species with three equal intensity carbonyl resonances at δ 188.4, 212.4, and 222.6, corresponding to a terminal and two semibridging carbonyls, respectively. Selective ^{31}P-decoupling experiments show that the three carbonyl resonances sharpen upon decoupling the high-field phosphorus resonance, but show little effect upon decoupling of the low-field resonance, suggesting that all three carbonyls are primarily bound to the same metal. Furthermore, the greater propensity of Ru to retain carbonyls and to adopt an 18-electron configuration,[64] as demonstrated for subsequent compounds in this report, leads us to make the structural assignment shown for **6** in Scheme 1. This, of course, leads to the assignment of the higher field ^{31}P resonance as due to the Ru-bound ^{31}P nuclei. In a sample of **6** that is ^{13}CO enriched, the high-field ^{13}C resonance and the one at δ 212.4 show mutual coupling of 21 Hz, suggesting that these carbonyls are mutually trans, and in the $^{13}CH_3$-enriched sample the methyl signal appears as a triplet ($^2J_{PC}$ = 8 Hz), with coupling to the Ir-bound phosphine. The ^{19}F NMR spectrum of **6** displays two resonances, one for the free triflate anion at δ −78.9 and one for a coordinated triflate anion at δ −77.5, indicating that a triflate anion has replaced one of the carbonyl groups originally bound to Ru, maintaining the 18-electron configuration at this metal. The methyl resonance appears in the ^1H NMR spectrum as a triplet at δ 1.58, showing coupling to only the Ir-bound ^{31}P nuclei. In Scheme 1 we show an Ir^{1+}/Ru^{2+} formulation, similar to that described for complex **4**.

The transformations involving the BF_4^- salt of **3**, as the temperature was warmed above −90 °C, were not followed in the absence of CO. In the presence of CO, warming generated the BF_4^- salt of **5**.

In attempts to learn more about the methyl-bridged species, **3**, we also investigated the protonation of the PMe_3 analogue

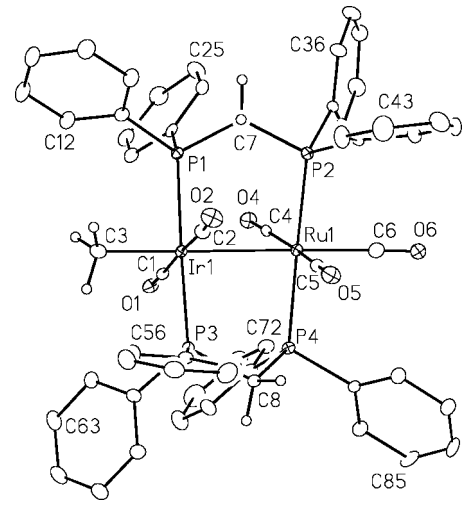

Figure 1. Perspective view of the complex cation of $[IrRu(CH_3)(CO)_5(dppm)_2][CF_3SO_3]_2$ (**5**) showing the atom-numbering scheme. Non-hydrogen atoms are represented by Gaussian ellipsoids at the 20% probability level. Hydrogen atoms are shown with arbitrarily small thermal parameters except for phenyl hydrogens, which are omitted. Ir−Ru = 2.9143(5) Å.

(63) Johnson, K. A.; Gladfelter, W. L. *Organometallics* **1990**, *9*, 2101.

(64) Parkin, G. *Comprehensive Organometallic Chemistry III*; Crabtree, R. H. Mingos. D.M. P., Eds.; Elsevier Ltd.: Oxford, 2007; Vol 1.

Scheme 2

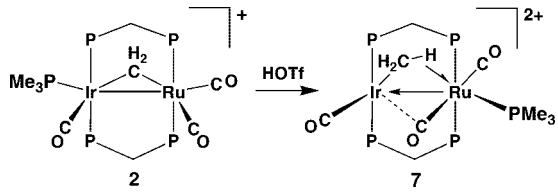

of **1**, namely, $[IrRu(PMe_3)(CO)_3(\mu\text{-}CH_2)(dppm)_2][CF_3SO_3]$ (**2**), as shown in Scheme 2. By substituting a carbonyl in **3** by a bulkier phosphine ligand we hoped to inhibit methyl migration to Ir and its accompanying partial "merry-go-round" motion of the other ligands in the Ir−Ru−CH_3 plane. This approach had been successful in the analogous Rh/Os system, in which the methyl-bridged tetracarbonyl species was stable only below −40 °C,[31] whereas the phosphine-substituted products $[RhOs(PR_3)(CO)_3(\mu\text{-}CH_3)(dppm)_2][CF_3SO_3]_2$ were isolable at ambient temperature.[32] We also reasoned that the greater basicity of the metals, resulting from substitution of CO by PMe_3, could lead to protonation directly at the metals and might favor a methylene/hydride product.

Protonation of **2** at ambient temperature generates $[IrRu(PMe_3)(CO)_3(\mu\text{-}CH_3)(dppm)_2][CF_3SO_3]_2$ (**7**), in which an unsymmetrically bridged methyl group again results, apparently via direct protonation at the methylene group. At temperatures below −60 °C two separate signals, in a 2:1 ratio, are observed in the ^1H NMR spectrum as broad singlets at δ 2.93 and −9.09, respectively, much as was observed for **3** at a somewhat lower temperature. Compound **7** is also obtained by protonation at −90 °C with no other species being observed. With broadband phosphorus decoupling, these signals resolve into a broad doublet and a triplet, having mutual coupling of 13 Hz. A bridging agostic methyl group is again proposed for **7**, on the basis of the mutual 13 Hz coupling between the hydrogens, as noted above, which is too large for a methylene/hydride structure, and also on the basis of the individual C−H coupling constants for the agostic and terminal hydrogens, as described in what follows. In a sample of **7**, prepared from the $^{13}CH_2$-enriched **2**, the low-field proton signal displays additional 140 Hz coupling to carbon, while the high-field signal displays 72 Hz coupling. As noted for **3**, the former coupling is typical for the terminal protons of a CH_3 moiety,[8,54] while the latter represents an agostic interaction.[46,47] Although the C−H coupling constant for the agostic interaction is greater than that for **3**, it is nevertheless still very small. As noted earlier, the observation of two resonances for the methyl protons is unusual. Exchange of these agostic and terminal C−H groups is usually too rapid, even at low temperatures, giving rise to only one average signal for the CH_3 group; certainly this was the case for the analogous Rh/Os[31,32] and Rh/Ru[30] species, for which only a single ^1H resonance for the methyl group was observed in each case.

A spin-saturation-transfer experiment at −60 °C indicates that exchange of the methyl protons is occurring at this temperature, and a $\Delta G^{\ddagger}$ of 51.5 kJ mol^{-1} has been calculated for this exchange based on an EXSY experiment.[65] This rotation barrier is slightly higher than that of 41.0 kJ mol^{-1} (acquired at −40 °C and at 90 MHz), reported by Grubbs and co-workers,[55] for proton exchange in a mixed Ti/Rh complex containing an unsymmetrically bridged methyl group.

Selective ^{31}P-decoupling of the ^1H signals of **7** at temperatures below −60 °C indicates that the pair of low-field methyl protons are coupled to the Ir-bound ^{31}P nuclei at high-field, while the high-field methyl proton, assigned to that involved in the agostic interaction, is coupled to the Ru-bound ^{31}P nuclei. This defines the methyl group as being carbon-bound to Ir while bridging to Ru through the agostic interaction. The $^{13}C\{^1H\}$ NMR spectra, with selective ^{31}P decoupling, indicate that the carbonyl resonances at δ 203.5 and 184.6 are Ru-bound, while the third at δ 177.4 is Ir-bound, and in the isotopomer that is enriched in both $^{13}CH_3$ and ^{13}CO, the methyl group and the Ir-bound carbonyl show mutual coupling of 20 Hz, suggesting a mutually trans arrangement of these groups. In the $^{31}P\{^1H\}$ NMR spectrum at −80 °C, the PMe_3 resonance appears as a broad, partially resolved quintet, displaying coupling to all dppm phosphorus nuclei, whereas the Ir- and Ru-bound ^{31}P resonances of the dppm groups display 8 and 6 Hz coupling, respectively, to the PMe_3 group. On this basis, the location of the PMe_3 group is not clearly defined. This is not the first time that we have observed approximately equal coupling of a terminally bound ligand to both the adjacent and remote dppm phosphorus nuclei,[56,66−68] and in fact this was also observed for the precursor, **2**, the structure of which was unambiguously established by X-ray crystallography.[56] However, it can be established with some confidence that the PMe_3 group is bound to Ru on the basis that this phosphine displays 6 and 18 Hz coupling to the Ru-bound carbonyls, suggesting an arrangement in which it is cis to both carbonyls with the smaller coupling constant being to the one that is adjacent to the Ir metal center; no coupling to the Ir-bound carbonyl is observed.

As shown in Scheme 2, protonation has resulted in PMe_3 migration from Ir to Ru. As such, the structure of **7** resembles the Rh/Ru[30] and Rh/Os[31] analogues more than it does compound **3**, having a more coordinatively saturated environment at the group 8 metal instead of the more symmetric arrangement of **3**. Nevertheless, the bridging methyl group is C-bonded to Ir in both **3** and **7**.

Warming **7** to ambient temperature results in no significant change in most of the $^{31}P\{^1H\}$, $^{13}C\{^1H\}$, and ^1H NMR spectral parameters, suggesting no significant structural changes occur over this temperature range. However, a somewhat different picture emerges upon monitoring the spectral parameters for the methyl group. Warming **7** above −60 °C results in a broadening of both methyl signals in the ^1H NMR spectrum, and by −40 °C both have disappeared into the baseline. Surprisingly, no coalesced signal appears until near ambient temperature, at which point a signal at δ 0.2 appears. This chemical shift is more in line with a terminal methyl group than the value expected for the weighted average of the two low-temperature signals (ca. δ −1.1). Furthermore, in the $^{13}CH_3$ isotopomer the C−H coupling constant at ambient temperatures is 133 Hz, again corresponding to a terminally bound methyl group. Our failure to observe a coalesced signal at lower temperature and the discrepancies between the ambient and low-temperature spectra suggest a more complicated fluxional process than merely exchange of agostic and terminal methyl protons. Fortunately, the ^{13}C NMR spectrum gives additional spectral information about the transformation of the methyl ligand. At −80 °C the ^{13}C NMR spectrum appears as a triplet of doublets having the appropriate coupling to the inequivalent protons ($^1J_{CH}$ = 140, 72 Hz). Warming results in broadening and coalescence of the signal, and by −20 °C it appears as a

(65) Perrin, C. L.; Dwyer, T. J. *Chem. Rev.* **1990**, *90*, 935.

(66) Anderson, D. J. Ph.D. Thesis, University of Alberta, 2007.

(67) Rowsell, B. D.; Trepanier, S. J.; Lam, R.; McDonald, R.; Cowie, M. *Organometallics* **2002**, *21*, 3228.

(68) Oke, O.; McDonald, R.; Cowie, M. *Organometallics* **1999**, *18*, 1629.

Scheme 3

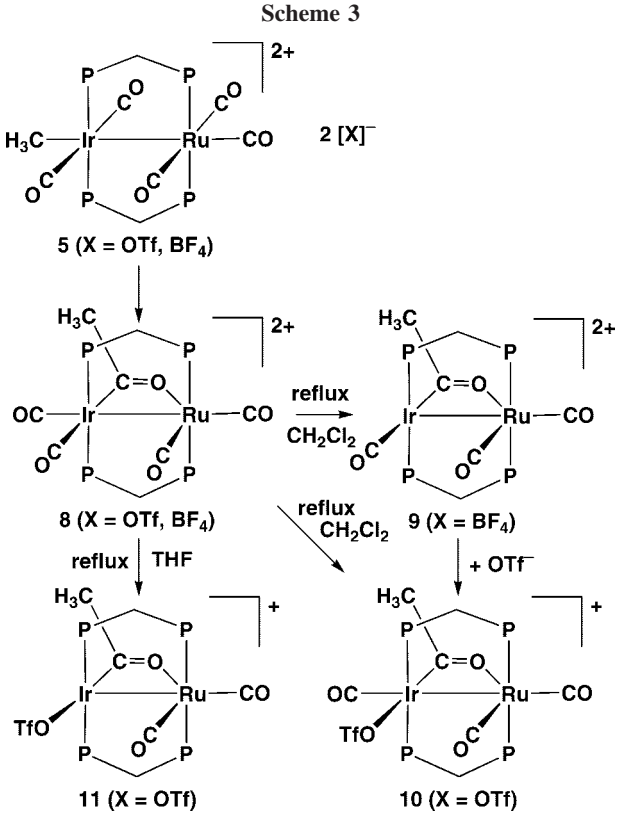

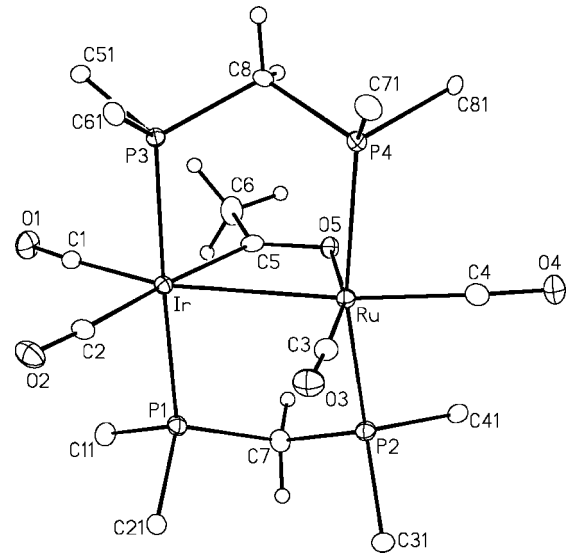

Figure 2. Perspective view of the complex cation of $[IrRu(CO)_4(\mu\text{-}C(CH_3)O)(dppm)_2][BF_4]_2$ (**8-BF$_4$**) showing the atom-labeling scheme. Thermal parameters as described for Figure 1. Only the ipso carbons of the dppm phenyl groups are shown. Relevant parameters (distances in Å and angles in deg): Ir−Ru = 2.8599(6), Ir−C(5) = 2.060(6), C(5)−O(5) = 1.250(8), Ru−O(5) = 2.137(4), Ir−C(5)−O(5) = 119.7(5), Ir−C(5)−C(6) = 125.9(5), C(6)−C(5)−O(5) = 114.4(6), C(5)−O(5)−Ru = 105.6(4).

quartet having the 117 Hz coupling to the three methyl protons. This coupling is exactly the weighted average of the two values obtained at lower temperature, consistent with rapid exchange of the agostic and terminal protons at −20 °C. Further warming again results in broadening of this signal, but by ambient temperature this resonance has sharpened into a quartet with 133 Hz C−H coupling. This significantly larger coupling is characteristic of a terminal methyl group, indicating that at this temperature the agostic interaction with Ru no longer persists. On the basis that all other spectral parameters are close to those at −80 °C, we propose that at ambient temperature the structure of **7** is much as it appears in Scheme 2, except without the agostic interaction.

Surprisingly, the chemical shift of the methyl carbon varies very little (δ 12.8 to 13.0) between −80 °C and ambient temperature, respectively. It is significant to note that as observed in the Rh/Os and Rh/Ru analogues, substitution of a carbonyl by a monophosphine ligand inhibits the "merry-go-round" motion of the equatorial ligands, so that monophosphine analogues of **4** are not observed.

(b) Acetyl-Bridged Complexes. As was the case for the PR_3 adducts of the methyl-bridged Rh/Os compounds,[32] compound **7** does not undergo subsequent migratory insertion, even at ambient temperature, although this species does begin to decompose to a complex mixture of uncharacterized products after several hours at this temperature. In contrast, the pentacarbonyl methyl complex **5** slowly transforms in solution over several days into a single acetyl-bridged product, $[IrRu(CO)_4(\mu\text{-}C(CH_3)O)(dppm)_2][CF_3SO_3]_2$ (**8**), as shown in Scheme 3. Unlike the three methyl complexes (**4**−**6**), for which the methyl resonances in the ^{1}H NMR spectrum appear as triplets, displaying coupling to two adjacent, metal-bound ^{31}P nuclei, the methyl resonance of **8** shows no ^{31}P coupling, appearing instead as a singlet at δ 2.43, suggesting that it is not bound to either metal. Five carbonyl resonances are observed in the $^{13}C\{^1H\}$ NMR spectrum; two at δ 204.6 and 187.5 are Ru-bound, while two at δ 172.4 and 157.7 are Ir-bound, as established by ^{31}P-decoupling experiments. The fifth low-field resonance at δ 251.2 is typical of an acyl group.[63,69−71] We were unable to obtain suitable crystals of **8** as the triflate salt; however, crystals of the BF_4^- salt (**8-BF$_4$**) were obtained. Spectroscopically, the parameters for the complex cations of both salts are indistinguishable. The structure of **8-BF$_4$**, shown in Figure 2, confirms the acetyl group formulation and establishes its bridging geometry, being carbon-bound to Ir and oxygen-bound to Ru. A similar bridging arrangement of acetyl groups was observed in the related Rh/Os[31] and Rh/Ru[30] chemistry, and again the acyl carbon was bound to the group 9 metal with the oxygen bound to the group 8 metal. Bridging acetyl groups were also observed in closely related Rh_2[71] and Ru_2[63,70] complexes. Each metal in **8** displays a distorted octahedral environment in which one site on each is occupied by the metal−metal bond. In each case the distortion results from the constraints arising from the bridging acetyl group, in which the acute Ru−Ir−C(5) and Ir−Ru−O(5) angles of 65.7(2)° and 69.0(1)°, respectively, differ substantially from the idealized value of 90°. The short Ir−C(5) distance (2.060(6) Å) and the long C(5)−O(5) distance (1.250(8) Å) suggest some degree of oxycarbene character, but this appears to be much less pronounced than was observed for the related metal−metal bonded Rh/Os[31] and Rh/Ru[30] systems, in which Rh−C distances were near 1.91 Å and C−O distances were near 1.27 Å. The lower degree of carbene character in the present case is consistent with the higher field ^{13}C signal for the acyl group than those previously reported.

Refluxing a solution of the BF_4^- salt of **8** in dichloromethane results in the loss of an iridium-bound carbonyl, yielding

(69) Jeffrey, J. C.; Orpen, A. G.; Stone, F. G. A.; Went, M. J. *J. Chem. Soc., Dalton Trans.* **1986**, 173.
(70) Gao, Y.; Jennings, M. C.; Puddephatt, R. J. *Organometallics* **2001**, *20*, 1882.
(71) Shafiq, F.; Kramarz, K. W.; Eisenberg, R. *Inorg. Chim. Acta* **1993**, *213*, 111.

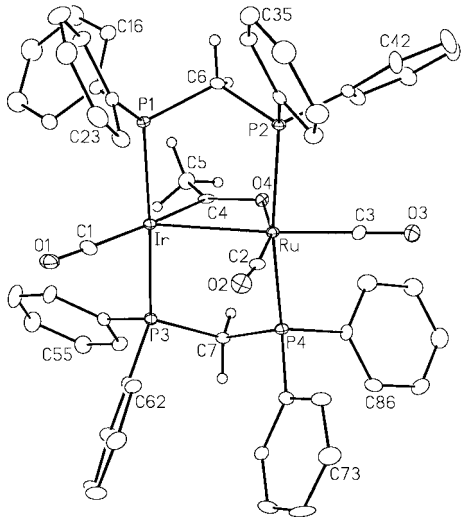

Figure 3. Perspective view of the complex cation of $[IrRu(CO)_3(\mu\text{-}C(CH_3)O)(dppm)_2][BF_4]_2$ (**9**) showing the atom-labeling scheme. Thermal parameters are as described for Figure 1. Relevant parameters (distances in Å and angles in deg): Ir−Ru = 2.7949(7), Ir−C(4) = 2.028(8), C(4)−O(4) = 1.285(8), Ru−O(4) = 2.132(5), Ir−C(4)−O(4) = 119.9(4), Ir−C(4)−C(5) = 123.0(6), C(5)−C(4)−O(4) = 117.1(7), Ru−O(4)−C(4) = 103.0(4).

$[IrRu(CO)_3(\mu\text{-}C(CH_3)O)(dppm)_2][BF_4]_2$ (**9**). The methyl group appears in the ^1H NMR spectrum as a singlet at δ 2.02, suggesting that the acetyl group has remained intact upon carbonyl loss, and this is supported by the very low-field resonance (δ 287.0) for the acyl carbonyl in the $^{13}C\{^1H\}$ NMR spectrum. Three other carbonyl resonances are observed at δ 179.8, 189.0, and 206.0, with the high- and low-field signals corresponding to the pair of Ru-bound carbonyls, while the intermediate signal corresponds to the Ir-bound carbonyl, as determined by selective ^{31}P-decoupling experiments. As we have previously noted, the lower field carbonyl resonance on a given metal usually corresponds to the group that is in the immediate vicinity of an adjacent metal.[62] It appears that for terminal carbonyls bound in a site near the adjacent metal, weak interactions with this metal (even though not structurally obvious) can lead to a downfield shift of this resonance. The IR spectrum displays three bands corresponding to the terminal carbonyls, but no carbonyl stretch is seen for the bridging acetyl group. We have been unable to unambiguously identify the carbonyl stretch for the bridging acyl group in any of the compounds in this paper or in our previous reports.[30,31] The X-ray structure determination of **9** confirms the proposed structure, as shown in Figure 3. Apart from a few minor differences, the structure of **9** appears very similar to that of **8**, in which the Ir-bound carbonyl opposite the metal−metal bond has been removed. Removal of the carbonyl has resulted in a shortening of the Ir−acyl bond (from 2.060(6) to 2.028(8) Å) and a corresponding lengthening of the acyl C−O bond (from 1.250(8) to 1.285(8) Å), indicating a shift from the conventional acyl extreme (**C**) toward the oxycarbene formulation (**D**). This proposed transformation is also consistent with the significant downfield shift of the ^{13}C resonance of this group, as noted earlier.

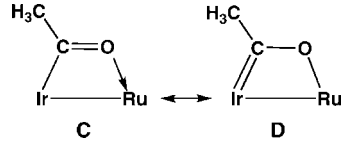

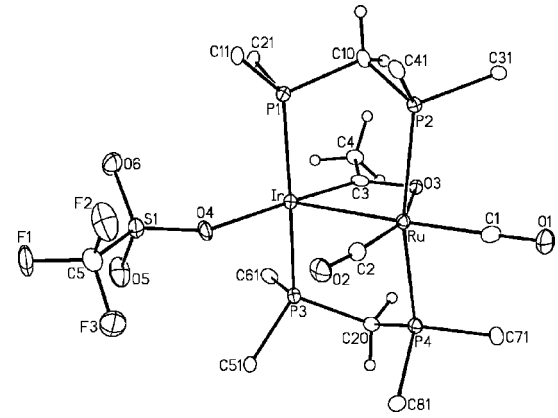

Figure 4. Perspective view of the complex cation of $[IrRu(OSO_2CF_3)(CO)_2(\mu\text{-}C(CH_3)O)(dppm)_2][CF_3SO_3]$ (**11**) showing the atom-labeling scheme. Thermal parameters as described for Figure 1. Only the ipso carbons of the dppm phenyl rings are shown. Relevant parameters (distances in Å and angles in deg): Ir−Ru = 2.7037(6), Ir−C(3) = 1.919(7), C(3)−O(3) = 1.292(8), Ru−O(3) = 2.123(4), Ir−C(3)−O(3) = 120.4(5), Ir−C(3)−C(4) = 125.0(5), C(4)−C(3)−O(3) = 114.6(6), C(3)−O(3)−Ru = 101.0(4).

If the triflate salt of **8** (instead of the BF_4^- salt) is refluxed in CH_2Cl_2, the carbonyl loss noted above is accompanied by triflate coordination at Ir, yielding $[IrRu(OSO_2CF_3)(CO)_3(\mu\text{-}C(CH_3)O)(dppm)_2][CF_3SO_3]$ (**10**), as demonstrated by resonances in the ^{19}F NMR spectrum corresponding to free (δ −78.9) and coordinated (δ −77.8) triflate ion. The formulation shown for **10** in Scheme 3 is based upon selective ^{31}P-decoupling experiments, through which it was established that the high-field carbonyl resonance in the $^{13}C\{^1H\}$ NMR spectrum corresponds to the one bound to Ir, while the other two carbonyls are Ru-bound. Furthermore, the very high-field chemical shift for the Ir-bound carbonyl (δ 168.6) suggests that it is in a position remote from the adjacent metal.[62] Similarly, the low-field Ru-bound carbonyl (δ 205.6) is assigned to the one that occupies the site adjacent to Ir, while the intermediate signal corresponds to the Ru-bound CO opposite the metal−metal bond. Upon triflate ion coordination, the acyl-carbonyl resonance has moved to significantly higher field (to δ 231.4 from 287.0), suggesting that this group is a normal bridging acyl group having little carbene character.

Refluxing the triflate salt of compound **8** in THF results in the loss of *two* carbonyls, yielding the acetyl-bridged dicarbonyl product $[IrRu(OSO_2CF_3)(CO)_2(\mu\text{-}C(CH_3)O)(dppm)_2][CF_3SO_3]$ (**11**). In the ^1H NMR spectrum the acetyl methyl group appears as a singlet at δ 1.57. The acyl carbonyl appears at δ 231.4 in the $^{13}C\{^1H\}$ NMR spectrum, displaying coupling to the Ir-bound phosphorus nuclei, while the carbonyl ligands appear at δ 186.7 and 205.6, and both show coupling to the pair of Ru-bound phosphorus nuclei. The lower field carbonyl signal corresponds to the one that approaches the bridging site between the metals. ^{19}F NMR spectroscopy displays two signals of equal intensity, and these are assigned to a coordinated and free triflate ion (δ −78.1 and −78.9, respectively). It is assumed that the coordinated triflate ion is bound to Ir, completing its coordination geometry.

An X-ray structural determination of **11**, shown in Figure 4, confirms the above structural assignment. This structure closely resembles that of **9**, in which the Ir-bound carbonyl has been replaced by a triflate anion. Although most differences between the two compounds are minor, the Ir−Ru bond (2.7037(6) Å) in **11** is the shortest in this series of acetyl-bridged species. In addition, the Ir−C(3) bond (1.919(7) Å) involving the acyl group

Scheme 4

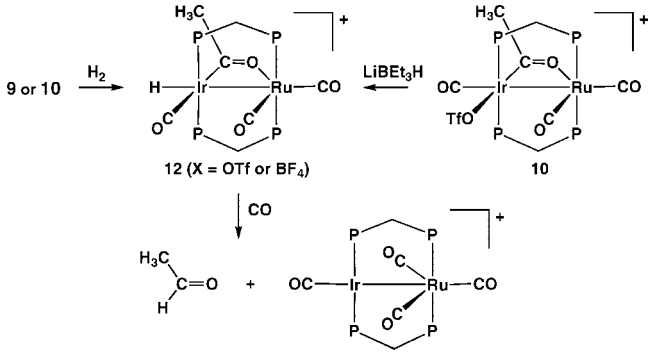

is extremely short and is comparable to the Rh−acyl distances in a series of related Rh/Os and Rh/Ru compounds, and the C(3)−O(3) bond (1.292(8) Å) is longer than those previously noted. Both parameters suggest a tendency toward the oxycarbene formulation **D**, although the ^{13}C resonance for this group, as noted above, is not unusual for an acyl group and does not by itself suggest the carbene formulation.

(c) Reactions with H_2. In our previous studies on the Rh/Ru[30] and Rh/Os[31] systems we had attempted the reactions of the acetyl-bridged complexes with H_2. Although we anticipated acetaldehyde as the probable product, we had wondered whether the oxycarbene-like nature of these groups (at least in their structural and spectroscopic characteristics) might give rise to unexpected reactivity, generating, for example, a hydroxycarbene group by hydrogen transfer to oxygen instead of to the acyl carbon. Unfortunately, the Rh-containing systems showed no reactivity with H_2 over the short-term. After several days small amounts of methane were detected, presumably by slow reversion to a methyl species, which then reacted with H_2. One reason for investigating the Ir/Ru system was the anticipation that oxidative addition of H_2 at Ir would be more favorable, and this has proven to be the case for at least three of the acetyl-bridged products.

Reaction of either $[IrRu(CO)_3(\mu\text{-}C(CH_3)O)(dppm)_2][BF_4]_2$ (**9**) or $[IrRu(OSO_2CF_3)(CO)_3(\mu\text{-}C(CH_3)O)(dppm)_2][CF_3SO_3]$ (**10**) with H_2 at ambient temperature yields the monohydride products $[IrRuH(CO)_3(\mu\text{-}C(CH_3)O)(dppm)_2][X]$ (**12**; X = CF_3SO_3, BF_4) as outlined in Scheme 4. The ^1H NMR spectrum of **12** (reported as the triflate salt) displays a hydride signal at δ −10.35 with coupling to only the iridium-bound phosphorus nuclei, suggesting that it is terminally bound to this metal. The acetyl protons appear as a singlet at δ 1.22, while the dppm methylene protons appear at δ 3.95 (all with the appropriate integrations). When a ^{13}CO-enriched sample of **12** is prepared, starting from **9(13CO)** or **10(13CO)**, the ^{13}C NMR spectrum shows the acyl carbonyl at typically low field (δ 260.2). Through a series of $^{13}C\{^{31}P\}$ NMR experiments, two carbonyls at δ 212.0 and 188.0 are assigned as being terminally bound to Ru, while the third, at δ 183.4, is terminally bound to Ir. A mutual coupling of 30 Hz between the acyl carbonyl and the highest field carbonyl suggests that they are mutually trans. By performing the reaction of **10** with dihydrogen at lower temperatures we hoped to observe intermediates in the formation of **12**. However, this was not the case. Compound **12** was the only species observed at −40 °C; below this temperature, no reaction was observed with either **9** or **10**. This monohydride product can also be formed more directly through addition of 1 equiv of superhydride ($LiBEt_3H$) to **10** at ambient temperature, further supporting its formulation. The formation of the monohydride (**12**) from either **9** or **10** appears to result from heterolytic cleavage of H_2 in which a hydride is delivered to the complex. Presumably, facile deprotonation of an unobserved dihydrogen complex by the counterion (triflate or fluoroborate) occurs, although no evidence of the corresponding acids was observed in the ^1H NMR spectra down to −80 °C. The acidity of dihydrogen complexes is well documented.[72]

Although reactions of **9** or **10** with H_2 did not yield acetaldehyde, the subsequent reaction of **12** with CO does generate this product together with the previously characterized $[IrRu(CO)_4(dppm)_2][OTf]$[56] and small amounts of uncharacterized dppm-containing products. The 0.2 equiv of acetaldehyde observed is significantly lower than anticipated, presumably through its loss due to displacement under the stream of CO gas.

The dicarbonyl species **11** also reacts with hydrogen gas, even at −90 °C, yielding what we propose to be the dihydrogen adduct $[IrRu(H_2)(CO)_2(\mu\text{-}C(CH_3)O)(dppm)_2][CF_3SO_3]_2$ (**13**), as shown in Scheme 5. We assume that in this product the dihydrogen ligand replaces the triflate ion of the precursor since no coordinated triflate is observed in the ^{19}F NMR spectra. $^{31}P\{^1H\}$

NMR spectroscopy shows that compound **11** is in equilibrium with **13**, with the ^{31}P integrals showing a 1:1 ratio of these compounds at a H_2 pressure of approximately 1 atm. The $^{31}P\{^1H\}$ NMR spectrum of **13** displays only one broad unresolved signal in which the resonances for the Ir- and Ru-bound ends of the diphosphines are coincidentally overlapping at δ 16.0. The resonance for the H_2 ligand is observed in the ^1H NMR as a broad signal at δ −0.03. This H_2 ligand is extremely labile, so warming a mixture of **11** and **13** above −90 °C results in a decrease in the concentration of **13**, and by −80 °C none of **13** remains.

In attempts to obtain the H−D coupling constant for the HD isotopomer of **13**, the H_2 ligand was displaced by passing HD through a sample at −90 °C. Although the substitution appeared to succeed, as witnessed by the 50% reduction in the intensity of the peak attributed to the H_2 ligand, while the ratio of **11** and **13** did not change appreciably in the ^{31}P NMR spectrum, we were unable to observe the expected coupling (ca. 30 Hz)[72] owing to the breadth of this signal (ca. 120 Hz at half-height). Unfortunately, T_1 measurements, although supportive of a dihydrogen complex, are also inconclusive owing to the instability of **13** at temperatures above −90 °C. One indication of an H_2 complex is a short $(T_1)_{min}$, generally below 100 ms (at 200 MHz).[72] For compound **13** the relaxation time (at 200 MHz) is found to be 112 ms at −90 °C. However, we suggest that the true $(T_1)_{min}$ is probably significantly less than this. In general, T_1 and T_2 are comparable and both decrease with decreasing temperature in what is referred to as the "extreme narrowing" region.[73] However, T_1 reaches a minimum, after which it increases with decreasing temperature while T_2 continues to decrease. The large discrepancy in T_1 and T_2 values for compound **13**, for which T_2 = 2.7 ms, suggests that we are at too low a temperature, so increasing the temperature (which is not possible for **13**) would be required to obtain $(T_1)_{min}$.

Upon warming above −60 °C homolytic cleavage of H_2 occurs, yielding the dihydride species $[IrRu(OSO_2CF_3)(H)_2(CO)_2(\mu$-

(72) (a) Kubas, G. J. *Comprehensive Organometallic Chemistry III*; Crabtree, R. H.; Mingos. D. M., Eds.; Elsevier Ltd.: Oxford, 2007; Vol. 1., Chapter 1.24. (b) Kubas, G. J. *Proc. Natl. Acad. Sci. U.S.A.* **2007**, *104*, 6901. (c) Heinekey, D. M.; Oldham, W. J. *Chem. Rev.* **1993**, *93*, 913. (d) Jessop, P. G.; Morris, R. H. *Coord. Chem. Rev.* **1992**, *121*, 155.

(73) Harris, R. K. *Nuclear Magnetic Resonance Spectroscopy−A Physicochemical View*; Longman Scientific and Technical: Harlow, Essex, UK, 1994.

Scheme 5

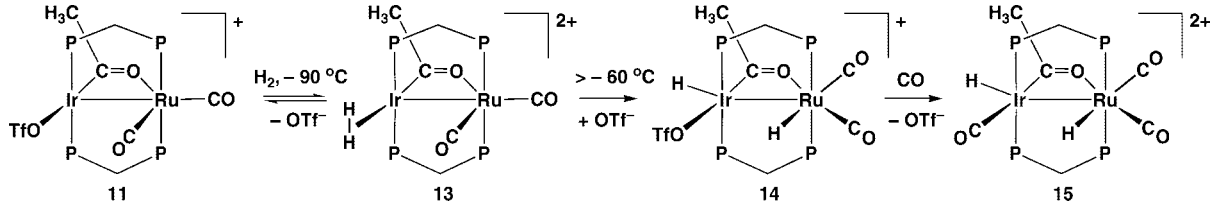

$C(CH_3)O)(dppm)_2][CF_3SO_3]$ (**14**). The ^1H NMR spectrum of **14** shows two hydride signals, one at δ −12.28, which shows coupling to the Ir-bound phosphorus nuclei, and the other at δ −9.95, which shows coupling to the Ru-bound phosphorus nuclei, suggesting that both hydrides are terminally bound to different metals. In addition, both hydrides display mutual coupling of 5 Hz, which is presumably transmitted via the metal−metal bond. The hydride at δ −9.95 shows additional coupling of 15 Hz to the Ru-bound carbonyl trans to it when a ^{13}CO-enriched sample is used; furthermore, in this isotopomer, the Ir-bound hydride at δ −12.28 displays no coupling to the acyl carbon, suggesting that they are mutually cis. The acetyl methyl signal appears at δ 0.94 in the ^1H NMR spectrum. The $^{13}C\{^1H\}$ NMR spectrum displays a triplet at δ 235.6 with 5 Hz coupling to the Ir-bound phosphorus nuclei. The relatively high-field shift of this acyl group is very similar to that of the starting dicarbonyl compound, **11**, suggesting an acyl structure closer to representation **C**. The two carbonyl ligands are shown to be terminally bound to ruthenium and appear at δ 192.8 and 191.8; the lack of coupling between them suggests that they are mutually cis. ^{19}F NMR spectroscopy shows two signals; one at δ −78.9 is assigned to the free triflate counterion and another at δ −79.5 is attributed to the bound triflate anion. It is assumed that this anion is coordinated to Ir since Ru is coordinatively saturated.

The instability of compound **13** above −90 °C casts some doubt on whether this species is the immediate precursor to the dihydride **14** (Scheme 5) or whether another, unobserved H_2 complex is involved.

Surprisingly, compound **14** does not give rise to detectable amounts of acetaldehyde, either when left in solution or when reacted with CO. Under an atmosphere of CO, triflate-ion displacement by CO occurs, yielding $[IrRu(H)_2(CO)_3(\mu\text{-}C(CH_3)O(dppm)_2][CF_3SO_3]_2$ (**15**), which also is stable for extended periods of time and does not yield detectable quantities of acetaldehyde. NMR spectroscopy (with appropriate heteronuclear decoupling experiments) supports the structure for **15** in which the coordinated triflate ion in **14** has been replaced by CO.

Conclusions

Reactivity at adjacent metal centers is inherently more complicated than that occurring at a single metal. Even for the simplest "multimetal" system—that containing only two metals—the different elementary steps in chemical transformations can, in principle, occur at either or both metals. The present study was initiated to determine how an Ir/Ru-based system might differ from analogous Rh/Ru[30] and Rh/Os[31] systems, with a view to establishing the roles of the different metals in substrate activation and subsequent transformations.

As is outlined in this paper, some reactivity differences between the Ir- and Rh-based systems were predictable on the basis of well-established differences in these metals, although others were unexpected. In the overall conversion of a bridging methylene group to a bridging acetyl group, through protonation followed by ligand migration and migratory insertion, the three systems behaved quite similarly. In all cases (Rh/Ru,[30] Rh/Os,[31] and Ir/Ru) protonation of the μ-CH_2 moiety gave an unsymmetrically bridged methyl group at low temperature, which migrated to a terminal site on the group 9 metal, followed by migratory insertion at that metal to give the bridging acetyl group. The low-temperature NMR studies on the three metal combinations, in which only the methyl-bridged products are observed, suggest direct protonation at the methylene group, rather than prior protonation at the metals followed by migration to the methylene carbon. Although we cannot rule out that the latter process is extremely facile and not observed, the failure to observe the methylene/hydride intermediate at −90 °C for all three metal combinations suggests to us that a metal hydride is not involved.

Notably, there are some subtle, although significant differences between the Rh- and Ir-based systems. First, the unsymmetrically bridged methyl group is σ-bound to Ir while involved in an agostic interaction with Ru in the current study, whereas for the Rh-based systems, the reverse is true, with the σ-bond being to the group 8 metal. Certainly, in this study the greater strength of the Ir−C bond compared to Ru−C or Rh−C[61] must be a dominant factor in this observation. In addition, the two compounds containing bridging methyl groups in this study were highly unusual in having very slow (on the NMR time scale) exchange between the "terminal" and "agostic" methyl hydrogens at low temperature, allowing the two different C−H coupling constants to be measured. As a consequence, these coupling constants for the agostic interactions in both species (65 and 72 Hz) are believed to be the lowest yet observed for unsymmetrically bridged methyl groups. Stronger interactions (lower $^1J_{CH}$ values) have been observed in mononuclear, electron-poor systems and in substituted bridging alkyl fragments.[47]

A further (predictable) difference between the Ir- and Rh-based systems is the rate of migratory insertion, which is orders of magnitude slower at Ir than at Rh, again in keeping with the stronger bonds involving the former. It may seem unusual that migratory insertion did not occur at the (presumed) more labile Ru center in the current study. However, in this system the methyl group is primarily bound to Ir and is involved with Ru only through a labile agostic interaction at very low temperature.

Although acetyl-bridged complexes are well precedented, an aspect of note is the irreversibility of their formation. In mononuclear chemistry, conversion of an alkyl/carbonyl species to the corresponding acyl product upon addition of CO or another Lewis base is generally reversed upon removal of a ligand. This did not occur in the chemistry described herein or in our previous studies.[30,31] Removal of up to two carbonyl ligands in this Ir/Ru system left the bridging acetyl group intact. One major difference between terminal and bridging acetyl groups is that in the former this group functions as a one-electron donor. Removal of a carbonyl (or other ligand) from the complex leads to deinsertion in order to satisfy the electronic requirement of the metal, regenerating a methyl and a carbonyl ligand, which

together supply three electrons to the metal, thereby compensating for the lost ligand. In the bridging mode, the acetyl group functions as a three-electron donor, so from the perspective of electron counting, nothing is gained upon deinsertion. In the binuclear system stabilization of an unsaturated species cannot be achieved through deinsertion and must be accommodated for in other ways by interactions with the adjacent metal or its ligands. Of course, anion coordination can also serve this function.

In investigating the Ir/Ru system we had hoped to exploit one major difference between Rh and Ir, namely, the greater tendency of the latter to undergo oxidative addition. This was certainly observed in the reaction with H_2; whereas both Rh systems were unreactive to H_2, the three Ir/Ru compounds investigated reacted readily with H_2. Both heterolytic and homolytic cleavage of H_2 were observed. In reactions with the cationic tricarbonyl precursors $[IrRu(OSO_2CF_3)(CO)_3(\mu\text{-}C(CH_3)O)(dppm)_2][CF_3SO_3]$ (**10**) and $[IrRu(CO)_3(\mu\text{-}C(CH_3)O)(dppm)_2][BF_4]_2$ (**9**), the only products observed were the monohydrides, $[IrRu(H)(CO)_3(\mu\text{-}C(CH_3)O)(dppm)_2][X]$ ($X = BF_4$, CF_3SO_3), whereas reaction of the dicarbonyl analogue $[IrRu(OSO_2CF_3)(CO)_2(\mu\text{-}C(CH_3)O)(dppm)_2][CF_3SO_3]$ (**11**) at −90 °C yielded a dihydrogen complex, which underwent homolytic H_2 cleavage to yield a dihydride at somewhat higher temperatures. The tendency of the first two species to undergo heterolytic cleavage is consistent with these species being more electron poor (one additional π-acceptor CO ligand) than **11**, therefore more acidic.[72]

The present study, together with previous work,[30,31,56,67,74] demonstrates that relatively simple differences, such as exchange of one metal (in this case Rh) by its heavier congener, can lead to unexpected differences in reactivity. It appears that in binuclear systems, subtle synergies between adjacent metals can play as important a role in the chemistry as do the well-established reactivity differences upon descending a triad. We continue to investigate such differences in attempts to elucidate the roles of the adjacent metals in this chemistry.

Acknowledgment. We thank the Natural Sciences and Engineering Research Council of Canada (NSERC) and the University of Alberta for financial support of this research, and NSERC for funding the Bruker PLATFORM/SMART 1000 CCD diffractometer and the Nicolet Avator IR spectrometer.

Supporting Information Available: CIF files giving crystal data for compounds **5**, **8**, **9**, and **11**. Tables of selected interatomic distances and angles for compounds **5**, **8**, **9**, and **11**. This material is available free of charge via the Internet at http://pubs.acs.org.

OM900127U

(74) (a) Trepanier, S. J.; Dennett, J. N. L.; Sterenberg, B. T.; McDonald, R.; Cowie, M. *J. Am. Chem. Soc.* **2004**, *126*, 8046. (b) Cowie, M. *Can. J. Chem.* **2005**, *83*, 1043.